Chemie der Erde 77 (2017) 303–321

Contents lists available at ScienceDirect

Chemie der Erde

journal homepage: www.elsevier.de/chemer

Geochemical characteristics of stream sediments from an urban-volcanic zone, Central Mexico: Natural and man-made inputs

V.C. Shruti[a], M.P. Jonathan[a,*], P.F. Rodríguez-Espinosa[a], R. Nagarajan[b], D.C. Escobedo-Urias[c], S.S. Morales-García[d], E. Martínez-Tavera[a]

[a] Centro Interdisciplinario de Investigaciones y Estudios sobre Medio Ambiente y Desarrollo (CIIEMAD), Instituto Politécnico Nacional (IPN), Calle 30 de Junio de 1520, Barrio la Laguna Ticomán, Del. Gustavo A. Madero, C.P. 07340, Ciudad de Mexico (CDMX), Mexico

[b] Department of Applied Geology, School of Engineering and Science, Curtin University, CDT 250, Miri, 98009, Sarawak, Malaysia

[c] Centro Interdisciplinario de Investigación para el Desarrollo Integral Regional (CIIDIR), Instituto Politécnico Nacional (IPN), Bulevar Juan de Dios Bátiz Paredes #250, Colonia San Joachin, Guasave, C.P. 81101, Sinaloa, Mexico

[d] Centro Mexicano para la Producción más Limpia (CMPL), Instituto Politécnico Nacional (IPN),Av. Acueducto s/n, Col. Barrio la Laguna Ticomán, Del. Gustavo A. Madero, C.P. 07340 Ciudad de México (CDMX), Mexico

ARTICLE INFO

Article history:
Received 9 September 2016
Received in revised form 2 March 2017
Accepted 21 April 2017
Editorial handling - Carita Augustsson

Keywords:
Fluvial sediments
Chemical weathering
Pollution indices
Volcano
Puebla
Mexico

ABSTRACT

Geochemical characteristics of stream sediments [n = 31; Upstream section: Zahuapan River (1–12) and Atoyac River (13–20); Downstream section (21–31)] from Atoyac River basin of Central Mexico have been evaluated. The study focuses on the textural, petrography and chemical composition of the fluvial sediments with the aim of analyzing their provenance, the chemical weathering signature and their potential environmental effects. The fluvial sediments are mostly composed of sand and silt sized particles dominated by plagioclase, pyroxenes, amphiboles, K-feldspar, biotite, opaque and quartz. The sediments were analyzed for determination of major (Al, Fe, Ca, Mg, Na, K, P, Si, Ti), trace elements (As, Ba, Be, Co, Cr, Cu, Mo, Mn, Ni, Pb, Sc, V, Y, Zn, Zr, Ga) and compared with Upper continental crust (UCC), source area composition and local background values. The elemental concentrations were comparable with the average andesite and dacitic composition of the source area and the local background values except for enrichment of Cu (56.27 ppm), Pb (34 ppm) and Zn (235.64 ppm) in the downstream sediments suggesting a significant external influence (anthropogenic). The fluvial sediments of Atoyac River basin display low CIA and PIA values implying predominantly weak to moderate weathering conditions in the source region. Based on the provenance discrimination diagrams and elemental ratios, it is understood that the collected sediments are derived from intermediate to felsic volcanic rocks dominated in the study region. Metal contamination indices highlight the enrichment of Cu, Pb, Zn, Mo, Cr and S clearly indicating the influences from natural (weathering and volcanic activity) and external (anthropogenic) sources. Ecological risk assessment results indicate that Cr, Ni and Zn will cause adverse biological effects to the riverine environment.

© 2017 Elsevier GmbH. All rights reserved.

1. Introduction

Fluvial systems are the most important dynamic systems, wherein their interaction with continental crust causes constant recycling of the materials of the Earth's crust. In that, rivers are the prime carrier of sedimentary materials from continents to the oceans, which result from continental denudation *i.e.*, the synergetic action of rock weathering and erosion. The deposited sediments preserve the imprints of all the processes in the passage from source to the sink. The geochemical composition of deposited stream sediments provide important information about their origins and can be therefore used to infer weathering trends, provenance of the sediment, depositional environment and sources of pollution in the region (Calvert et al., 2001; Glasby et al., 2004; Naimo et al., 2005; Wei et al., 2006; Liu et al., 2013).

Geochemical compositions of the fluvial sediments reveal the average composition of an entire drainage basin (Young et al., 2013). It is well-known that chemical weathering exerts a major control on sediment composition strongly affecting the elemental geochemistry and mineralogy of sediments (Johnsson and Meade, 1990; Van Loon and Mange, 2007; Schneider et al., 2016), where larger cations (Al_2O_3, Ba, Rb) remain fixed in the weathering profile

* Corresponding author.
E-mail address: mpjonathan7@yahoo.com (M.P. Jonathan).

http://dx.doi.org/10.1016/j.chemer.2017.04.005
0009-2819/© 2017 Elsevier GmbH. All rights reserved.

preferentially over smaller cations (Ca, Na, Sr) which are selectively leached (Nesbitt et al., 1980). These geochemical signatures are ultimately retained in the sediments thus inferring the provenance as well as the source area weathering conditions (e.g., Nesbitt and Young, 1982; Bhatia, 1983; Wronkiewicz and Condie, 1987; Cullers et al., 1988; Feng and Kerrich, 1990; Fedo et al., 1996; Armstrong-Altrin et al., 2015; Nagarajan et al., 2014).

Atoyac River, a major river of south-central Mexico flowing through states of Tlaxcala and Puebla is delimited by tectonic features like Volcano Iztaccíhuatl, Popocatépetl (active) in the western side, and Volcano Malinche in the eastern side. The research area has witnessed potential industrial (textile, petrochemicals, rubber etc.) and economic development favoring a demographic growth of 154.6% during the last two decades (INEGI, 2010). It is one of the most contaminated rivers of the country (CONAGUA, 2010) influenced by the natural volcanic inputs in addition with wastewater discharges from urban, agriculture and industrial zones. The fluvial sediments of Atoyac River basin provides an opportunity to gain knowledge about the influence of different processes on sediment chemistry, which is used as a proxy in interpretation of provenance, weathering conditions, source rock characteristics and sources of pollution in this river basin.

We present in this paper the texture, petrography, major and trace element composition of sediments to reveal the provenance, weathering conditions and source rock characteristics. In addition, geochemical indices such as enrichment factor (EF), geoaccumulation index (I_{geo}), pollution load index (PLI) and ecological risk assessment have been calculated to identify any potential environmental effects.

2. Study area description

2.1. Regional setting

The Atoyac River basin, lying between 18°57′02″ N and 98°15′37″ W in Central Mexico, constitutes Zahuapan River and Atoyac River flowing through the rural, urban, agricultural, and industrial regions of Tlaxcala and Puebla City, where it finally drains into the Manuel Ávila Camacho dam (Fig. 1). This basin has an extension of 4395 km^2, flanked by volcanoes Iztaccíhuatl and Popocatépetl (active) in the western side and volcano Malinche in the eastern side. Zahuapan River is fed by the runoff from Sierra de Tlaxco in the north and several minor channels originating from inland waters and the La Malinche volcano. Atoyac River originates from the Sierra Nevada de Toluca as a result of snow melt on the northern rim of Iztaccíhuatl volcano. The downstream section in the study area includes the confluence of both the rivers near Santo Toribio Xicohtzingo entering into the plains of Puebla. The river basin experiences sub-humid climate with an average annual precipitation of 800 mm and temperature of 22 °C. The dry season corresponds to the months of March-May, the rainy season from June-September and winter during October-February (National Meteorological Service, 2010).

2.2. Geological setting

Geologically, Tlaxcala region belongs to "*Tlaxcala Block*" consisting of Tertiary volcano-lacustrine sequence, which includes well-bedded sandy to silty pyroclastic material and it is overlaid by ignimbrites (Erffa von et al., 1976; Castro-Govea and Siebe, 2007). Upper Cenozoic intermediate tuffs and 2.6 Ma old Andesitic Spills out crop towards the top of the section (Castro-Goeva, 1999; INEGI, 1981; Ramírez Rojas, 1986). The Puebla basin is located in the central part of the Trans Mexican Volcanic Belt and is surrounded by Neogene-Quaternary stratovolcanoes like Iztaccíhuatl (extinct), Popocatépetl (active since 1994) and Malinche (dormant) (Nelson and Sanchez-Rubio, 1986). The metamorphic Acatlán complex (Paleozoic) forms the basement rocks overlain by sedimentary carbonaceous deposits (cretaceous) and terrigenous deposits from Maltrata and Balsas formations (Siebe et al., 1996). The products of recent volcanic activity (Quaternary) as lava flows, pyroclastic deposits and laharic flows from Popocatépetl and Iztaccíhuatl are covering a part of the basin. Calc-alkaline, alkaline and numerous inter-layered pyroclastic deposits of andesitic to dacitic composition are also present in the study area (Schaaf et al., 2005; Larocque et al., 2008). The carbonate rocks in some sections are part of the mafic replenishment and magma mixing with andesitic-dacite origins (Goff et al., 2001). Pink Pumices of 1150 yr B.P and Tutti Frutti Pumice of 14,000 yr B.P of pyroclastic sequences is also present in the foot hills of the volcanoes (Siebe and Macías, 2004). The region is also fed by a number of small springs, which cuts through the quaternary gravels of different sequences overlying the Tertiary Balsas Conglomerate with modern terrestrial fresh water molluscs (shells) present in the region (Stevens et al., 2012).

2.3. Industrial set-up

The Puebla and Tlaxcala states are the fourth largest metropolitan area of Mexico and it forms the major industrial corridor in the center of the country. These states form the major grounds for automobile manufacturing and they are the prime sites for the origin of textile industry in Latin America, which favored an increase in the demographic growth (154.6%) during the last two decades (INEGI, 2010). On the industrial front, the State of Puebla and Tlaxcala are dominated with manufacturing units of aluminum, ceramic, food, transport sector, wooden materials, dyes, electrical, petrochemical, chemicals, adhesives, colorants, fertilizers, oil lubricants, synthetic and printing industries, rubber, textile, heavy machines and automobiles. These industrial complexes are easy sources for rapid discharge of industrial effluents into the fluvial systems.

3. Materials and methods

3.1. Sample collection

A total number of 31 surface sediment samples were collected from the main river channels, which includes Zahuapan River (sample nos. 1–12), Atoyac River (sample nos. 13–20) and downstream section (sample nos. 21–31) respectively (Fig. 1). The samples were divided into three sections based on the geomorphological and the drainage basin features in the mountainous terrain. The samples were collected using plastic spatula and a small Van-veen grab was also used where the depth (0.5–2.3 m) of water column was more. The samples were immediately packed and transferred to the lab, where the samples were oven dried at <40 °C. Larger particles (>256 mm) were eliminated manually before the pulverization process. The sediments (<2 mm) were pulverized using agate mortar and sieved through ASTM 200 sieves for geochemical study.

Some of the collected samples, especially 1–4 (Zahuapan River), 13, 14 (Atoyac River), were collected from the drainage basins (considered as non-polluted) in the mountainous region, where smaller springs feed the main rivers. The above mentioned samples were used as local reference values to estimate background values in the present study.

3.2. Grain size and petrographic analysis

The bulk sample was reduced to the known quantity by coning and quartering method and a portion (~100 g) of the sample was used for grain size analysis. Grain size analysis was conducted by the dry sieving technique (Folk, 1980). Samples containing

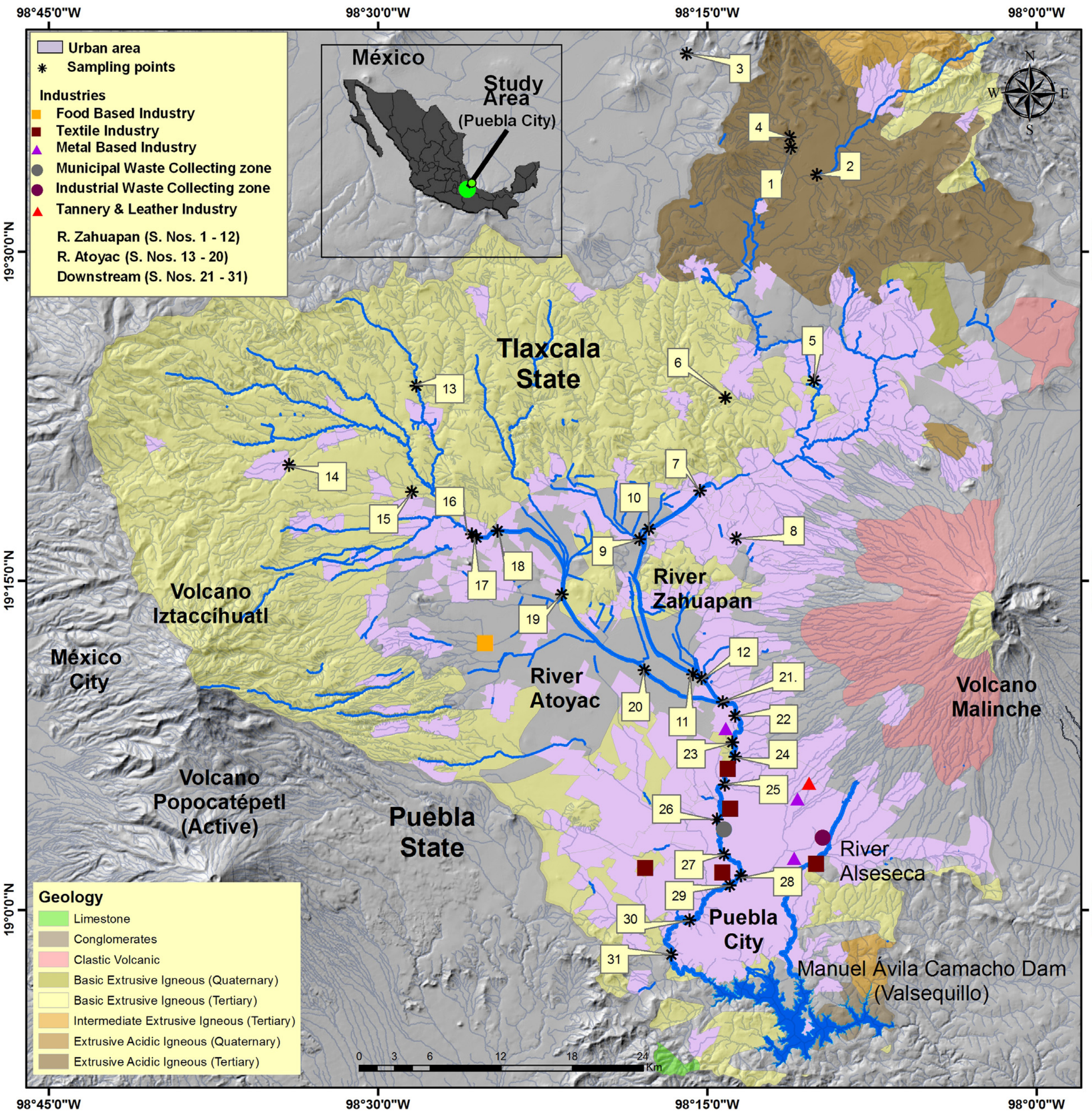

Fig. 1. Location and geology map of the study area showing sampling locations from Zahuapan River (sample nos. 1–12), Atoyac River (sample nos. 13–20) and Downstream side (sample nos. 21–31), Puebla, México.

more than 5% fine fraction (finer than 4ϕ) were analyzed using the pipette method as described by Griffiths (1951) and Carver (1971). Sediment textural classes were deduced according to Folk (1980). Various grain size parameters were computed based on using GRADISTAT software (Blott and Pye, 2001).

Petrographic investigations were carried out for twenty five (12 from Zahuapan River, 7 from Atoyac River and 6 from Downstream) sediment samples impregnated with the resin (2:2:1 ratio of resin, hardener and acetone respectively). The impregnated sediment samples were cut to the size of the glass slide of about 5 mm thickness using Lortone Lapidary Bench Trim Saw. Samples were subsequently grinded using Hillquist Thin Section Grinder with 45, 30 and 25 μm diamond flat lap surfaces of rotation speed (rpm) 45, 30 and 25 respectively until the smooth surface was obtained. The polished samples were further polished by using fine carborundum powder on a glass plate to attain a smooth surface and the samples were then fixed on the glass slides by heating Canada balsam without air bubbles. After drying, the samples were grinded using Hillquist Thin Section Grinder with 15 μm diamond flat tap until a desirable thickness was obtained. Meanwhile, the thin sections were observed under microscope from time to time in order to obtain an accurate thickness (30 μm) of grains all showing the correct order of interference colour. Lastly, the slides were polished with 600 and 1000 grit carborundum powder on a glass plate and few samples were further polished using 2000 grit powder. Petrographic examination were carried out at Curtin University, Sarawak using Nikon Eclipse LV100NPOL polarizing/reflecting microscope equipped with Nikon DSF12 camera. Measurement and photography studies were carried out under the microscope using NIS Elements Version 4.40 software and plagioclase composition was determined by the Michel-Levy method.

3.3. Geochemical analysis

Major (Al, Fe, Ca, Mg, Na, K, P, S, Ti) and trace elements (Ag, As, Ba, Be, Co, Cr, Cu, Mo, Mn, Ni, Pb, Sc, Sr, V, Y, Zn, Zr, Ga) were analyzed in ACT Labs, Ontario, Canada. 0.25 g of powdered sample (mesh size: 200 micros) were mixed with $HClO_4$–HNO_3–HCl–HF acids (all analytical grade) and was digested at 260 °C, which was subsequently made up with diluted HCl (0.1 M). Internal quality checks were done in a frequency of 20% and sample replicates (twice) were done with analytical blanks at regular intervals. The metal concentrations were determined using inductively coupled plasma-mass spectrometry (ICP-MS) and Geochemical Reference Standard Materials (SRMs: GXR-1; GXR-4) were run concurrently with the samples and the recoveries were between 83.11 and 110.5% and 87.26–107.4% for trace metals.

3.4. Statistical analysis

Statistical calculations for the present data set were performed using Statistica software (Version 8.0). The inter-relationship between the geochemical elements were identified using correlation analysis with $p < 0.05$ Factor analysis involving varimax normalization in order to minimize the number of variables with a high loading on each component was performed to ascertain the sources of contamination (natural and external). In addition, the factor analysis was also based on the eigen values (more than 1).

3.5. Weathering indices

Weathering indices such as chemical index of alteration [CIA = $100(Al_2O_3/Al_2O_3 + CaO^* + Na_2O + K_2O)$] and plagioclase index of alteration [PIA = $Al_2O_3 - K_2O/(Al_2O_3 + CaO^* + Na_2O - K_2O)] \times 100$, where CaO^* represents Ca in silicate-bearing minerals only (Nesbitt and Young, 1989) are widely used to interpret the weathering history of modern and ancient sediments. Since we did have the CO_2 data to compute CaO^*, the method proposed by Bock et al., 1998 was adopted. Accordingly, CaO values were accepted only if $CaO \leq Na_2O$, otherwise the CaO concentration was assumed to be equal to Na_2O (Bock et al., 1998). Unweathered rocks have CIA and PIA values of 50 and the degradation of feldspars increases the value up to 100.

The ternary plots A-CN-K and A-CNK-FM are used to deduce the silicate weathering trends (Fedo et al., 1995; Nesbitt and Young, 1984, 1989). The Index of Compositional Variability (ICV) = $[Fe_2O_3 + K_2O + Na_2O + CaO + MgO + MnO + TiO_2)/Al_2O_3]$ is used to assess the maturity of sediments (Cox and Lowe, 1995). The influence of sorting processes was deduced through Al_2O_3-TiO_2-Zr ternary plot by García et al., 1994.

3.6. Estimation of metal contamination

The most important factor in the interpretation of geochemical data is the choice of background value and the best alternative is to compare the concentrations between contaminated and uncontaminated sediments (Covelli and Fontolan, 1997; Rubio et al., 2000; Sakan et al., 2009). In this research work the background values were calculated from the mean concentrations of metals in uncontaminated sediments of the study area.

3.6.1. Enrichment factor (EF)

Enrichment factor (EF) is an effective tool in distinguishing metals originating from anthropogenic activities and those from natural crustal contribution (Buat-Ménard and Chesselet, 1979; Sakan et al., 2009; Armid et al., 2014; Chen et al., 2016). EF value between $0.5 - 1.5$ suggests that the metals may be entirely from the crustal materials or natural weathering processes, while EF > 1.5 indicates that a significant portion of metals is from other external sources rather than natural origins (Zhang and Liu, 2002). The enrichment is evaluated as follows: EF<1 indicates no enrichment; <3 is minor enrichment; 3–5 is moderate enrichment; 5–10 is moderately severe enrichment; 10–25 is severe enrichment; 25–30 is very severe enrichment and >50 is extremely severe enrichment.

3.6.2. Geoaccumulation index (I_{geo})

The geoaccumulation index (I_{geo}), proposed by Muller (1981) permits to assess the extent of sediment contamination which consists of seven classes. The I_{geo} ranges from class 0 (<=0: uncontaminated), class 1 (0–1: uncontaminated to moderately contaminated), class 2 (1–2: moderately contaminated), class 3 (2–3: moderately to strongly contaminated), class 4 (3–4: strongly contaminated), class 5 (4–5: strongly to extremely contaminated) and class 6 (> 5: extremely contaminated) which is atleast 100 fold enrichment above the background values (Bhuiyan et al., 2011; Kalender and Uçar, 2013).

3.6.3. Pollution load index (PLI)

The extent of pollution by trace metals was also assessed by employing PLI which provides a simple, comparative means for assessing a site where a value of 0, 1 and >1 indicates absence, presence and progressive deterioration of sediment quality, respectively (Tomlinson et al., 1980).

3.6.4. Potential ecological risk assessment

The possible ecological risks posed by the presence of metals in sediments were assessed though comparison with ecotoxicological values that include effect range low (ERL) and effect range median (ERM) (Long et al., 1995). The values below ERL suggest no biological effects whereas values above ERM indicate harmful effects on the biological community (USEPA, 2001; Long et al., 1995).

4. Results

4.1. Grain size and petrographic studies

4.1.1. Grain size parameters

The sediments of Atoyac River basin consist almost entirely of sand and silt sized particles. The mean size (M_z) of Zahuapan River sediments varies from very coarse sand to coarse silt i.e. −0.63 to 5.83 ϕ with an average of 2.38 ϕ (fine sand) (Table 1). Likewise, Atoyac River sediments varies from very coarse sand to very coarse silt (M_z = 0.10 to 4.23 ϕ) and downstream sediments are dominated by silt ranging between very coarse sand to medium silt (M_z = −0.67 to 6.47 ϕ). The kurtosis value ranges from 0.59 to 3.01 i.e. very platykutic to extremely leptokurtic strongly suggesting a fluvial environment, confirming that the sediments are deposited through various river depositional processes. The skewness ranges from very coarse skewed to very fine skewed (−0.55 to 2.54), thus indicating the presence of fine fraction and coarse fraction in population of river sediments. The Zahuapan River sediments are well sorted (avg. 2.20 ϕ), suggesting a lower energy state when compared to Atoyac and downstream section sediments which are poorly to very poorly sorted with values of 1.93 ϕ and 1.50 ϕ respectively indicating glacio-fluvial settings (Friedman, 1961; Blott and Pye, 2001; Okeyode and Jibiri, 2013).

4.1.2. Sediment mode of transportation

The cumulative curves plotted on the probability ordinate scale describes the type of sediment transport in the Atoyac River basin (Fig. 2). The different lengths and slopes of the cumulative curves are related to the modes of sediment transportation by traction, saltation and suspension (Visher, 1969). The fluvial samples show a similar pattern for Zahuapan River, Atoayac River and the

Table 1
Grain size analysis of the Atoyac River basin sediments, Puebla, Mexico.

Study area	Sample no.	Phi 5	Phi 16	Phi 25	Phi 50	Phi 75	Phi 84	Phi 95	Mean grain size
River Zahuapan	1	-3.4	-2.5	-1.3	3.2	6	8.1	8.7	2.93
	2	1.1	1.5	2	4.5	6.7	8	8.7	4.67
	3	-1.8	0	1.4	4.2	7	8.1	8.8	4.1
	4	2.1	3.1	3.6	6	8.1	8.4	8.8	5.83
	5	-2.4	0.2	1	1.9	2.4	2.7	2.9	1.6
	6	1	2	2.3	3	4	5.3	8.3	3.43
	7	-4.6	-3.8	-3.2	-1.4	0.5	1.3	2.7	-1.3
	8	-1.9	-1.3	-0.8	0.2	1.4	1.8	2.8	0.23
	9	2.1	3.1	3.5	5.1	7.4	8.2	8.8	5.47
	10	-3.5	-1.8	-1.5	-0.7	0.2	0.6	1.5	-0.63
	11	-0.9	-0.6	-0.4	0.2	0.7	0.9	1.4	0.17
	12	-1	0.4	1.2	2.3	3.2	3.5	3.9	2.07
River Atoyac	13	-1.9	0.8	1.9	3.2	4.4	5.7	8.4	3.23
	14	-4.6	-3.8	-3.1	-0.6	2.3	3.7	8	0.10
	15	1.6	2.2	2.3	2.7	3.1	3.5	3.8	2.80
	16	-0.9	-0.3	0.1	0.6	1.3	2.7	7.9	1.00
	17	-1.7	-1.3	-0.7	0.7	1.7	2.2	3	0.53
	18	-0.8	0.2	0.7	2.1	2.8	3.3	3.9	1.87
	19	-0.7	0.3	1.1	2.9	3.5	3.7	4	2.30
	20	2.4	3.2	3.4	3.8	4.8	5.7	8.3	4.23
Downstream side	21	-1.8	-1.4	-1	0.3	1.3	1.8	3.2	0.23
	22	4.2	4.3	4.4	4.5	4.8	4.9	5	4.57
	23	-4.5	-3.5	-2.6	0.1	1.1	1.5	2	-0.67
	24	-0.6	0.2	0.4	1.4	3	3.5	4.1	1.7
	25	2.2	2.8	3.3	6.1	7	8.2	8.7	5.7
	26	0.3	1	1.3	2.1	2.7	2.8	3.3	1.97
	27	-	-	-	-	-	-	-	-
	28	-3.70	-3.10	-2.60	-1.50	-0.30	0.40	1.60	-1.40
	29	4.3	4.9	5.1	5.6	6.7	8.2	8.7	6.23
	30	-	-	-	-	-	-	-	-
	31	4.5	5.1	5.3	5.8	8.3	8.6	8.8	6.47

downstream section. They are characterized by a well-developed traction/saltation population with 74.18, 65.01 and 58.49 percentage of distribution in the three zones respectively. The truncation between traction and saltation was between 3ϕ and 4ϕ. Truncation between saltation and suspension was at 8 ϕ with (Fig. 2) a percentage of 16.79, 31.73 and 32.23 for the three zones respectively. Likewise, suspension load ranged between 3.26 and 9.28%. Cumulative curves of the present study indicate that traction is the major process of transport though saltation and suspension have also played some role during the deposition of these sediments (e.g. Farhat and Salem, 2015).

4.1.3. *Petrography*

Texturally, the sediments are coarse to fine in nature and are dominated by fragments (lithic + volcanic glass) than the mineral grains. The mineral grains are dominated by plagioclase, pyroxenes (clino and ortho pyroxenes), amphiboles, K-feldspar, biotite, opaque, traces of altered olivine grains and quartz. Plagioclases constitute the major part of the mineral grains, which shows normal polysynthetic twinning and disequilibrium features such as complex zoning pattern and sieve texture (Fig. 3a), often filled with glassy inclusions (e.g. Nelson and Montana, 1992; Weidendorfer et al., 2014). The melt inclusions are elongated parallel to polysynthetic twin plan. Plagioclases with polysynthetic twinning dominate over zoned plagioclases and their composition mainly between albite to andesine. Lithic fragments are volcanic and pyroclastic in nature. Three major types of lithic are observed, such as porphyritic, aphyric and hypo-crystalline (Fig. 3b). Felty/hyalopilitic textures are also noticed in several lithics where microlites of plagioclase show random orientation (Fig. 3c). Glomeroporphyritc textures are also noticed in few lithics (e.g. Khalifa et al., 2011). Some of the samples show highly ferrugenised lithic fragments (sample 3; Fig. 3d) and are mostly sub-rounded, whereas mineral grains vary between anhedral to subhedral and rarely of euhedral crystals. Pyroclastic fragments are altered and exhibits grey and brown colour under plane polarized light. Most of the vitric and/or glass shards showed dirty brown to black colour, which are the matrix for any lithics (Fig. 3e) (e.g. Krippner et al., 1998). Pumice fragments are common and are mostly vitric to crystal tuff, some samples show lithic tuff and or ignimbrites lithics (Fig. 3f). Rhyolitic and dacitic tuffs are also observed along with andesitic fragments showing bimodal distribution of plagioclase phenocrysts. Porphyritic fragments show many phenocrysts, such as plagioclase, hornblende, pyroxenes (mostly clinopyroxene), biotite and opaque minerals (Fig. 3g). Hornblende phenocrysts in the lithics are rimmed by iron oxides and show corrosion features. Sanidine is common in some of the fragments but mostly less than plagioclases. Hornblende shows simple twinning, corrosion features within the lithic grain and are altered to opaque mineral. Biotite in the lithics also shows corrosion feature. Replacement of pyroxene by hornblende, hornblende by biotite, biotite by chlorite and plagioclase by epidote and clay are also noticed. Vitric banded lithics are also observed. Carbonates are not common in all the sediments, except one sample where carbonate grains is observed (Fig. 3i). Fe-Ti oxides are the most common accessory phase, occurring as microphone crysts and as small inclusions in the hornblende, pyroxene etc (e.g. Schmitz and Smith, 2004). Heavy minerals such as magnetites, sphene and zircon (trace) were noted in the lithic grains of some samples and likewise, bioclasts are common in few samples (Sample Nos. 5 and 12) (Fig. 3j). Overall the mineral grains, matrix and volcanic pyroclastic lithics are felsic to intermediate in nature. Similarly, glass and microlites acts as matrix and groundmass in the pyroclastic and volcanic fragments (e.g. D'Oriano et al., 2014).

4.2. *Geochemistry*

4.2.1. *Major elements*

The major elemental compositions in the fluvial sediments of Atoyac River basin are listed in Table 2. The concentration pat-

Table 2
Major and trace elemental concentrations in Atoyac River basin sediments, Puebla, México.

Study area	Sample Nos.	Al	Fe	Ca	Mg	Na	K	P	S	Ti	Ag	As	Ba	Be	Co	Cr	Cu	Mo	Mn	Ni	Pb	Sc	Sr	V	Y	Zn	Zr	Ga
Zahuapan River	1*	9.26	4.14	2.62	1.10	2.02	1.30	0.041	0.03	0.49	<0.3	< 3	492	2	21	135	22	3	780	65	< 3	12	384	91	17	59	135	30
	2*	9.29	3.66	2.76	0.87	2.19	0.99	0.042	0.03	0.26	<0.3	< 3	411	2	18	108	13	2	782	48	8	11	417	49	15	61	97	29
	3*	9.51	3.75	1.82	0.80	1.74	0.99	0.055	0.02	0.34	<0.3	4	443	2	14	114	19	5	526	33	6	12	345	58	15	88	134	32
	4*	8.48	3.09	2.63	0.85	2.03	1.11	0.032	0.03	0.39	<0.3	4	369	2	14	153	12	4	595	33	8	11	388	81	16	61	129	27
	5	7.83	6.30	4.59	1.92	2.70	1.41	0.079	0.16	0.20	<0.3	< 3	372	1	26	330	16	< 1	754	71	14	14	516	84	12	100	53	27
	6	9.47	3.31	3.49	1.32	2.85	1.24	0.026	0.02	0.48	<0.3	< 3	274	2	14	175	8	7	483	45	5	12	502	93	13	53	100	29
	7	8.29	3.35	3.33	1.42	3.25	1.67	0.057	0.07	0.28	<0.3	< 3	502	1	14	159	11	3	536	29	19	11	572	61	12	70	69	27
	8	8.34	3.42	3.80	1.45	3.09	1.29	0.090	0.15	0.40	<0.3	< 3	426	1	15	184	17	9	651	31	25	11	546	92	12	101	96	28
	9	9.14	3.61	2.98	0.95	2.09	1.11	0.048	0.34	0.43	0.5	9	394	2	14	83	34	4	540	36	22	12	418	95	18	124	136	29
	10	8.37	2.94	3.26	1.33	3.25	1.56	0.055	0.09	0.35	<0.3	< 3	430	1	15	189	9	7	500	24	8	10	554	82	13	67	89	26
	11	8.64	2.82	3.50	1.28	3.33	1.39	0.049	0.11	0.33	<0.3	4	445	1	18	156	9	9	544	25	15	10	604	81	13	67	79	26
	12	9.29	3.11	4.06	1.44	3.20	1.51	0.053	0.04	0.36	0.7	4	335	1	13	232	11	8	721	33	36	11	603	146	13	615	357	28
	Avg.(5-12)	8.67	3.61	3.63	1.39	2.97	1.40	0.06	0.12	0.35	0.38	4	397.25	1.25	16.13	188.50	14.38	6	591.13	36.75	18	11.38	539.38	91.75	13.25	149.63	122.58	27.50
Atoyac River	13*	9.29	2.87	3.44	1.28	2.91	1.35	0.031	0.03	0.41	<0.3	3	328	2	11	204	9	9	402	38	7	10	482	76	13	57	93	28
	14*	8.18	4.15	3.42	2.19	2.18	1.07	0.081	0.04	0.45	<0.3	< 3	351	1	24	212	14	5	1170	72	14	15	395	100	14	83	120	26
	15	8.97	3.39	3.89	1.71	2.90	1.42	0.041	0.04	0.42	<0.3	< 3	281	1	15	246	10	9	573	51	5	12	522	92	12	62	111	27
	16	9.03	3.20	3.31	1.25	2.69	1.34	0.064	0.15	0.34	<0.3	3	275	2	13	214	19	6	470	47	12	12	446	79	14	96	113	29
	17	7.26	4.47	3.63	2.87	2.73	1.32	0.072	0.08	0.47	<0.3	< 3	317	1	22	259	18	3	825	73	30	15	381	107	14	94	115	24
	18	7.81	4.47	3.43	2.41	2.62	1.14	0.060	0.13	0.24	<0.3	< 3	241	1	20	337	14	< 1	751	69	24	14	400	80	13	115	69	25
	19	8.53	3.26	3.31	1.55	2.82	1.41	0.050	0.16	0.37	<0.3	< 3	302	2	14	123	17	2	526	47	16	11	431	85	12	80	94	27
	20	7.65	2.86	3.06	1.47	2.65	1.47	0.083	0.27	0.28	<0.3	5	299	1	15	702	22	47	490	56	17	9	378	74	10	106	77	23
	Avg.(15-20)	8.21	3.61	3.44	1.88	2.74	1.35	0.06	0.14	0.35	0.30	3.33	285.83	1.33	16.50	313.50	16.67	11.33	605.83	57.17	17.33	12.17	426.33	86.17	12.50	92.17	96.50	25.83
Downstream side	21	6.84	4.65	3.43	2.62	2.75	1.23	0.078	0.12	0.53	<0.3	< 3	331	1	24	358	13	9	806	68	6	13	400	121	12	92	119	25
	22	7.35	3.97	3.40	1.27	2.25	1.32	0.150	0.48	0.4	1.7	14	389	1	14	127	72	3	632	38	61	11	418	110	13	336	102	25
	23	8.56	3.85	3.53	1.57	3.25	1.54	0.064	0.10	0.55	0.3	5	390	1	17	102	22	2	570	34	7	11	604	109	12	86	79	27
	24	8.74	3.48	3.97	1.88	3.10	1.36	0.069	0.21	0.40	<0.3	6	303	1	20	281	24	13	586	58	12	12	529	93	13	99	88	27
	25	6.05	2.53	12.8	1.30	1.96	0.78	0.159	0.47	0.30	0.4	4	212	<1	11	259	35	13	437	42	19	9	638	73	9	149	71	19
	26	7.01	3.53	4.12	2.47	2.98	1.09	0.057	0.10	0.36	<0.3	< 3	321	1	20	397	15	9	625	97	< 3	9	489	90	8	83	112	26
	27	2.42	1.22	20.4	0.75	0.69	0.33	0.255	0.82	0.08	1.1	5	149	<1	7	281	83	17	309	40	24	< 4	753	45	5	411	13	9
	28	7.56	3.72	5.69	1.91	2.90	1.53	0.147	0.19	0.37	1.1	3	443	1	17	182	76	6	624	65	147	12	518	97	13	119	101	25
	29	2.86	1.73	17	0.89	0.86	0.41	0.335	0.87	0.17	1.3	5	164	<1	11	104	110	7	317	46	32	4	635	54	6	475	13	9
	30	7.67	3.22	4.85	1.71	3.13	1.32	0.071	0.18	0.24	<0.3	6	244	1	17	139	18	2	544	43	12	10	538	63	10	112	68	23
	31	3.00	1.69	13.3	0.84	0.82	0.44	0.519	0.97	0.14	2.4	5	200	<1	12	487	151	28	399	57	51	4	508	62	7	630	13	10
	Avg.(21-31)	6.19	3.05	8.41	1.56	2.24	1.03	0.17	0.41	0.32	0.86	5.36	286	1	15.45	247	56.27	9.91	531.73	53.45	34	9	548.18	83.36	9.82	235.64	70.82	20.45
†Overall avg.		7.47	3.36	5.69	1.58	2.59	1.23	0.11	0.25	0.34	0.57	4.44	321.56	1.16	15.92	244.24	33.36	9	568.52	49	24.88	10.52	516.12	86.72	11.56	173.68	93.48	24
STD		1.96	1.02	4.75	0.55	0.77	0.36	0.11	0.27	0.12	-	2.47	92.13	-	4.30	138.55	36.43	9.87	135.40	17.65	29.06	2.89	93.75	22.01	2.81	172.59	63.82	5.95
NASC		8.94	3.95	2.59	1.72	0.84	3.30	0.06	-	0.42	-	28.4	6.36	-	25.7	125	-	-	0.05	58	-	14.9	142	130	35	-	200	-
UC		8	3.49	3.0	1.32	2.89	2.82	-	-	-	-	1.5	550	-	10	35	25	-	0.06	20	-	11	350	60	22	71	190	-
Wedephol (1995)		7.97	3.18	3.03	1.39	2.64	2.65	0.07	-	0.32	55	2	668	3.1	12	35	14	1.4	0.05	19	17	7	316	53	21	52	237	14

*1–4: Background Samples for Zahuapan River; *13–14: Background Samples for Atoyac River. † Overall avg. (Expect Background samples).
Major elements are represented in % and trace elements in ppm. NASC = Average North American Shale; UC = Upper Crust (data from Taylor and McLennan, 1985).

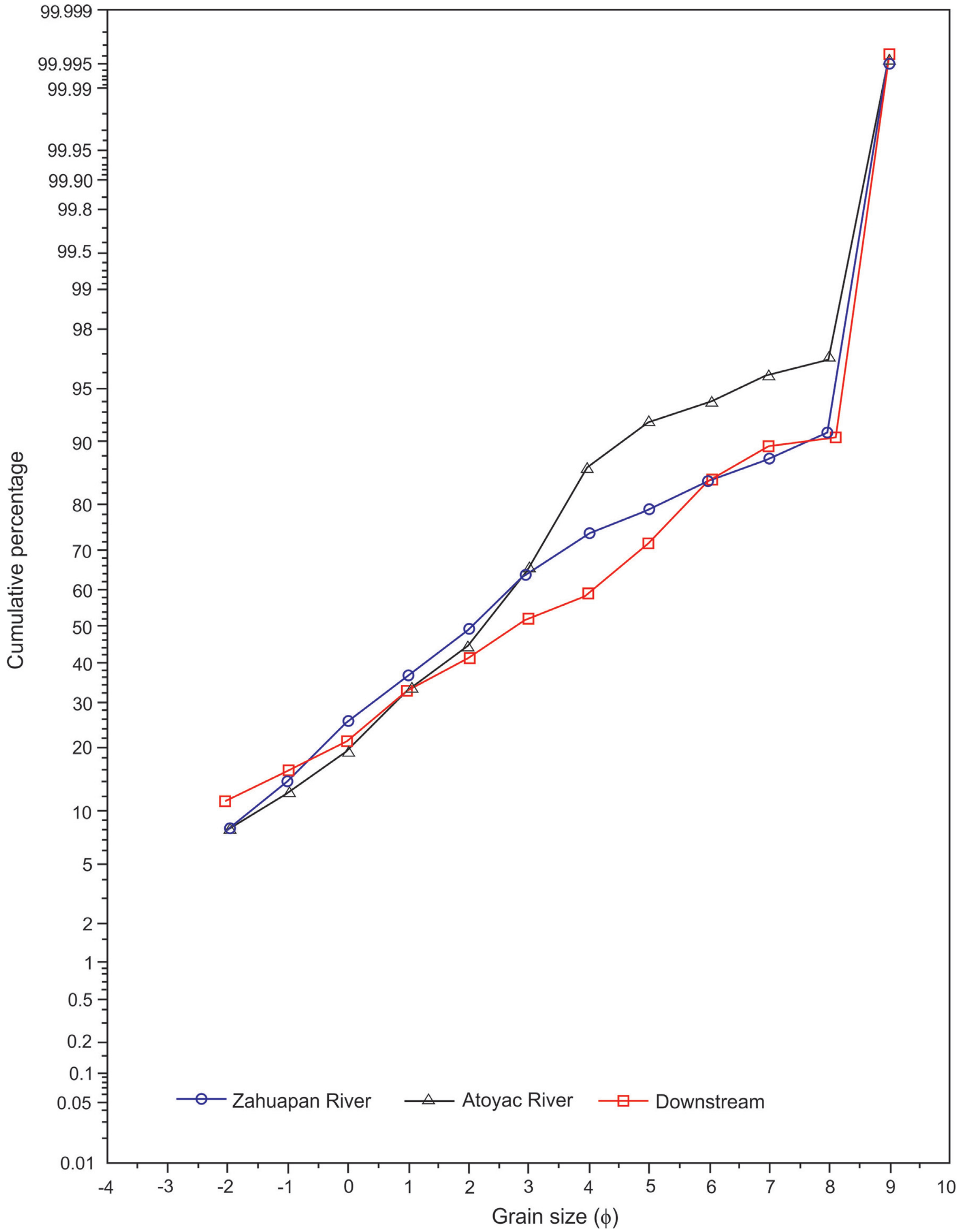

Fig. 2. Visher plot displaying different modes of sediment transport.

tern reveals that Al content in Zahuapan River and Atoyac River show minor variations (7.83–9.51 and 7.26–9.29%) than the downstream side (2.42–8.74%). Fe concentrations in the region show a decreasing trend towards the downstream section (3.05%) when compared with Atoyac River (3.61%). While, Ca content indicate a two-fold (8.41%) increase in the downstream sediments compared to Zahuapan River (3.63%) and Atoyac River (3.44%). Mg content in the sediments show higher values in Atoyac River (1.88%) than in Zahuapan River (1.39%) and downstream side (1.56%). Na and K content indicate higher values in Zahuapan River (2.97 and 1.40%) and Atoyac River (2.74 and 1.35%) than downstream (2.24 and 1.03%). P and S are recorded with higher concentrations (0.17 and 0.41%) in downstream side than in the upstream side.

4.2.2. *Trace elements*

The higher averages (in ppm) of trace elemental concentrations are recorded from Zahuapan River for Ba (397), V (92), Y (13), Zr (123), Ga (28); from Atoyac River for Be (1.33), Co (16.5), Cr (314),

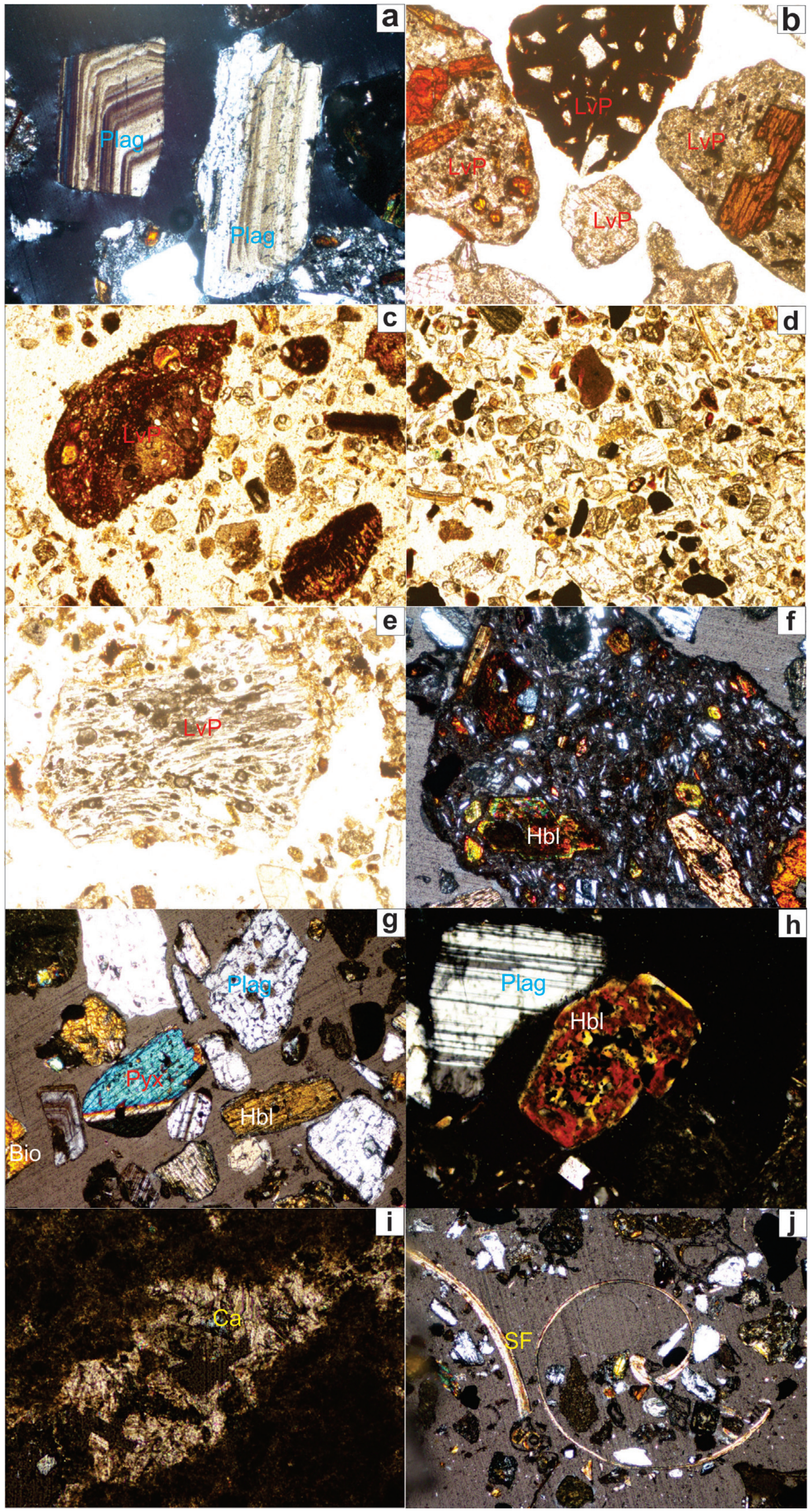

Fig. 3. a–j Thin-section photomicrographs of selected samples showing detrital modal compositions. a) plagioclase showing polysynthetic twinning; b) different types of lithic; c) Felty/hyalopilitic texture; d) Ferrugenised lithic fragments; e) Vitric/glass shards; f) lithic tuff or ignimbrites lithics; g) phenocrysts such as plagioclase, hornblende, pyroxenes, biotite and opaque minerals; i) carbonate grains and j) bioclasts.

Mo (11.33), Mn (606), Ni (57), and Sc (12.17) and from downstream for Ag (0.86), As (5.36), Cu (56), Pb (34), Sr (548), Zn (236) respectively (Table 2). In the downstream sediments an increasing trend for metals such as As, Cu, Pb and Zn are observed.

The elemental concentrations of Zahuapan, Atoyac Rivers and downstream sediments were normalized against UCC and local background values (Fig. 4a–b) in order to highlight the differences between the three zones. In comparison with UCC it is observed that Zahuapan River sediments are enriched in Cr, Mo, Sr, Zn and Ga and are depleted in other elements except Fe, Ca, Mg, Co, and Mn. Likewise, Atoyac River sediments are enriched in Ca, Mg, Cr, Mo, Mn, Ni, Sr Zn and Ga, and depleted in few elements. Downstream sediments show a different trend compared to Zahuapan River and Atoyac River sediments and are enriched in Ca, Mg, P, Cr, Cu, Mo, Ni, Pb, Sr, Zn and Ga. All the samples show depletion in the concentrations of K, Ba, Be, Y and Zr. All the elemental concentrations recorded in the studied sediments (except P, Pb content in the downstream sediments) are comparable with the average andesite and dacite composition from the source area (Fig. 4a) (Obenholzner et al., 2003). In comparison with local background values, Zahuapan River and Atoyac River sediments are equivalent except Mg, Ba, Ni, Cu, Pb, Zn, and Zr. The elements Ca, P, Cu, Pb and Zn are enriched in downstream sediments compared to other upstream river sediments, which can be related to the anthropogenic inputs from the study region (Fig. 4b).

5. Discussion

5.1. Geochemistry

The higher concentration of Ca in the downstream sediment (8.41%) suggests that it has been contributed from altered carbonates from volcanic and pyroclastic lithic fragments and bioclasts in addition to mafic igneous minerals rather than limestones or calcareous minerals, the later has less significant effect on the total Ca content of the samples. The average CaO reported for brown and white pumice from Popocatepetl volcanic eruption in 1997 was 6.30 and 5.34 wt% (Witter et al., 2005). The source of S in the sediments is from the mafic magmas of volcanic origin. The primitive lavas of this region contain high concentration of S which is readily available under high pressure conditions forming other metal complexes during early crystallization (Cervantes and Wallace, 2003; Schaaf et al., 2005). The higher averages of Cr, Cu, Ni, Zn and Mo in the fluvial sediments indicate that they are from the non-crystalized particles often discharged from active volcano Popocatépetl which is situated on the western side of the study area (Obenholzner et al., 2003), consisting mainly of andesite, dacite, and minor amount of basaltic andesite. Increasing trends for metals such as As, Cu, Pb and Zn in the downstream sediments are mainly sourced from the upstream side and the industrial input from the Puebla city limits. In addition, the higher values are also due to the precipitation of metal sulphides from the pumices (Larocque et al., 2008).

The correlations of individual geochemical elements were performed as one single analysis for each section with the p values at 0.05 (Table 3). The strong correlation of Al *vs* Na ($r^2 = 0.97$), K ($r^2 = 0.96$), Ti ($r^2 = 0.83$), Sc ($r^2 = 0.93$), Y ($r^2 = 0.88$), Ga ($r^2 = 0.98$), Fe ($r^2 = 0.87$), and Zr ($r^2 = 0.85$) in downstream sediments indicates that they are of detrital origin with the presence of either feldspar or heavy minerals (Cox and Lowe, 1995; Pe-Piper et al., 2005). The negative correlation of Al *vs* Ca ($r^2 = -0.92$), P ($r^2 = -0.84$), Cu ($r^2 = -0.77$), Sr ($r^2 = -0.51$), Zn ($r^2 = -0.85$), and Mo ($r^2 = -0.63$) suggests that these elements are associated with volcanic lithic fragments (carbonates and sulphates). The strong association of Al *vs* Ti and Y also supports that the sediments are detrital with phyllosilicates and mafic minerals (Ahmad and Chandra, 2013). Zone based analysis revealed that the ferromagnesium elements [Co ($r^2 = 0.83$, 0.90, 0.87), Cr ($r^2 = 0.57$), and Ni ($r^2 = 0.84$, 0.86)] are correlated with Fe rather than Mn, suggesting their bonding to Fe-oxides. The positive relationship of Cr *vs* Mo ($r^2 = 0.80$) and Ni ($r^2 = 0.62$) in downstream sediments indicates that these elements are from a similar source, which is mainly from metal based chemical industries, where they are widely used as anti-corrosive agent. Likewise, the positive relationship of Mo *vs* S dictates its presence as sulphur bearing minerals like pyrite. In Zahuapan River and Atoyac River sediments, the association of Ca with Mg ($r^2 = 0.92$, 0.11), Na ($r^2 = 0.72$, 0.58), K ($r^2 = 0.62$, 0.25), Cr ($r^2 = 0.82$, −0.44), and Sr ($r^2 = 0.78$, 0.79) indicate their association with plagioclase feldspars and Ca bearing pyroxenes and pyroclastic materials from the volcanic source region. It is derived from the volcanic activity which brought xenocrysts of carbonate and skarn from the bottom of the arc (Witter et al., 2005). In downstream sediments, the association of Ca with P ($r^2 = 0.72$), S ($r^2 = 0.86$), Cu ($r^2 = 0.65$), Mo ($r^2 = 0.56$), Sr ($r^2 = 0.77$) and Zn ($r^2 = 0.71$) infers that Ca is not mainly controlled by plagioclase feldspar but may be controlled by more than one source such as carbonate bioclastic materials and chalcophile elements under acidic conditions. The non-association of Cr, Pb and Ni with other geochemical elements suggests that these elements are due to the anthropogenic inputs especially from the electroplating industries (Hanif et al., 2016; Takarina, 2010).

Factor analysis was performed for all the three zones separately to identify the geochemical processes distinctly. The factor scores were derived based on the Eigen values (<1) for each zones. The cumulative factor scores (in%) for Zahuapan River, Atoyac River and downstream sediments were 90.61, 93.83 and 92.68 with 6, 5 and 4 factors, respectively (Table 4). The factor analysis results in the three zones clearly indicate the geochemical processes that control the chemistry of the sediments. The "Fe-Mn Factor" is represented by the positive loadings of Fe, Mn, Mg, P, Co, Ni, Sc, Pb, Cr in Factor 2 (Zahuapan River) and Factor 1 (Atoyac River and downstream sediments) indicating that they are adsorbed on to Fe-Mn oxides in the sediments. "Carbonate Mineral Factor" indicates positive values of Ca, Mg, Na, K, Cr, Pb, Sr, V, Zn, Zr in Zahuapan River (F1), Atoyac River (F3) and downstream sediments (F3) inferring that considerable weathering is taking place in the lower part of the region. The "Chalcophile-Anthropogenic Factor" is dominated by positive values of S, As, Cu, Mo, Cr and Cu in Zahuapan River (F4), Atoyac River (F2), downstream sediments (F2) indicating the presence of chalcophile elements and the influence of anthropogenic sources in the study area. The "Pb-Factor" is dominated by Pb, V, Zn, Zr, Cu in Zahuapan River (F3), downstream sediments (F4) indicating the natural influence (through detrital minerals) as well as anthropogenic source. Finally, the "P-Factor" is dominated mainly by P in Zahuapan River (F6) and Atoyac River (F5) indicating some organic material input in the upstream side of the rivers especially from the mountains and S due to the volcanic peaks and P from agricultural region in the downstream region.

5.2. Weathering and sorting characteristics

The calculated CIA (%) results for the present study were between 59 and 75 percentage (Zahuapan River: 59–75, Atoyac River: 61–68 and downstream sediments: 59–67), suggesting weak to moderate weathering in the source area (Fig. 5a). Low CIA values in the present study are attributed to the influx of less weathered detrital minerals from a tectonically active region and semi-arid conditions, which leads for mechanical erosion (e.g. Nehyba and Roetzel, 2015; Sharma et al., 2013). The PIA values of Zahuapan River (61–78), Atoyac River (60–70) and downstream sediments (60–70) suggest moderate degradation of plagioclase feldspar into clay minerals (Nesbitt and Young, 1982).

Table 3
Correlation analysis of Atoyac River basin sediments, Puebla, Mexico.

		Al	Fe	Ca	Mg	Na	K	P	S	Ti	As	Ba	Cd	Co	Cr	Cu	Mo	Mn	Ni	Pb	Sc	Sr	V	Y	Zn	Zr	Ga
River Zahuapan (n = 12)	Al	1.00	-	-0.55	-0.63	-0.46	-0.53	-0.60	-	0.52	-	-	-	-	-0.59	-	-	-	-	-	-	-	-	0.52	-	0.50	0.76
	Fe		1.00	-	-	-	-	-	-	-	-	-	-	0.83	0.57	-	-0.66	0.52	0.84	-	0.90	-	-	-	-	-	-
	Ca			1.00	0.92	0.72	0.62	0.50	-	-	-	-	-	-	0.82	-	-	-	-	0.56	-	0.78	0.52	-0.68	-	-	-0.62
	Mg				1.00	0.71	0.73	0.59	-	-	-	-	-	-	0.89	-	-	-	-	-	-	0.73	-	-0.77	-	-	-0.53
	Na					1.00	0.83	-	-	-	-	-	-	-	0.49	-0.60	0.57	-	-	0.50	-	0.98	-	-0.81	-	-	-0.73
	K						1.00	-	-	-	-	-	-	-	0.55	-	-	-	-	-	-	0.82	-	-0.64	-	-	-0.66
	P							1.00	-	-	-	-	-	-	0.50	-	-	-	-	-	-	-	-	-0.52	-	-	-
	S								1.00	-	0.77	-	-	-	-	0.69	-	-	-	-	-	-	-	-	-	-	-
	Ti									1.00	-	-	-	-	-	-	-	-	-	-	-	-	-	-	-	-	-
	As										1.00	-	-	-	-	0.76	-	-	-	-	-	-	-	0.63	-	-	-
	Ba											1.00	-	-	-	-	-	-	-	-	-	-	-	-	-	-	-
	Cd												1.00	-	-	-	-	-	-	-	-	-	-	-	-	-	-
	Co													1.00	0.51	-	-0.51	0.61	0.81	-	0.57	-	-	-	-	-	-
	Cr														1.00	-	-	-	-	-	-	0.53	-	-0.68	-	-	-
	Cu															1.00	-	-	-	-	-	-0.54	-	0.70	-	-	0.50
	Mo																1.00	-	-0.66	-	-0.60	0.54	-	-	-	-	-
	Mn																	1.00	0.68	-	-	-	-	-	-	-	-
	Ni																		1.00	-	0.81	-	-	-	-	-	-
	Pb																			1.00	-	0.59	0.64	-	0.76	0.58	-
	Sc																				1.00	-	-	-	-	-	-
	Sr																					1.00	-	-0.79	-	-	-0.72
	V																						1.00	-	0.81	0.77	-
	Y																							1.00	-	-	0.50
	Zn																								1.00	0.93	-
	Zr																									1.00	-
	Ga																										1.00
River Atoyac (n = 8)	Al	1.00	-0.64	-	-0.77	0.54	-	-0.72	-	-	-	-	-	-0.74	-0.50	-0.63	-	-	-0.86	-	-0.50	0.82	-	-	-	-	0.92
	Fe		1.00	-	0.95	-0.51	-0.75	-	-	-	-0.50	-	-	0.90	-	-	-0.51	0.74	0.86	-	0.94	-0.50	-	0.54	-	-	-
	Ca			1.00	-	0.58	-	-	-0.75	-	-	-	-	-	-	-0.69	-			-	0	0.79	0.80		0.63	0.73	-
	Mg				1.00	-	-0.58	-	-	-	-	-	-	0.89	-	-	-	0.69	0.87	-	0.85	-0.51	-		-	-	-0.61
	Na					1.00	0.81	-0.67	-	-	.-	-	-	-0.73	-	-	-	-0.59	-0.78	-	-0.54	0.78	-		0.58	0.57	-
	K						1.00	-	-	-	0.53	-	-	-0.75	-	-	-	-0.68	-0.73	-	-0.76	0.54	-	-0.55	0.42		-
	P							1.00	0.50	-	0.41	-	-	0.65	0.53	0.75	-	0.54	0.66	-	-	-0.64	-				-0.64
	S								1.00	-0.67	0.59	-	-	-	0.70	0.86	0.66	-	-	-	-	-0.54	-0.51	-0.63	-0.23		-0.50
	Ti									1.00	-0.45	0.68	-	-	-0.54	-	-	-	-	-	-	-	–	0.50	-0.13		-
	As										1.00		-	-	0.84	-	0.90	-	-	-	-0.60	-	-	-0.72	0.39		-
	Ba											1.00	-	-	-	-	-	-	-	-	-	-	0.50		-		-
	Cd												1.00	-	-	-	-	-	-	-	-	-	-		-		-
	Co													1.00	-	-	-	0.88	0.94	-	0.87	-0.59	-		-		-0.58
	Cr														1.00	0.53	0.91	-	-	-	-	-	-	-0.70	-		-0.72
	Cu															1.00	0.50	-	-	-	-	-0.68	-	-	-		-0.52
	Mo																1.00	-	-	-	-0.63	-	-	-0.80	-		-0.51
	Mn																	1.00	0.67	-	0.81	-	-	0.50	-		-
	Ni																		1.00	-	0.77	-0.79	-	-	-0.50	-0.51	-0.70
	Pb																			1-.00	-	-	0.71	-	0.71	0.62	
	Sc																			-	1.00	-	-	0.73	-	-	
	Sr																					1.00	0.61	-	0.71	0.78	0.68
	V																						1.00	-	0.86	0.92	-
	Y																							1.00	-		-
	Zn																								1.00	0.96	-
	Zr																									1.00	-
	Ga																										1.00

Downstream (n = 11)	Al	1.00	0.87	-0.92	0.70	0.97	0.96	-0.84	-0.91	0.83	-	0.79	-	0.74	-	-0.77	-0.63	0.78	-	-	0.93	-0.51	0.76	0.88	-0.85	0.85	0.98
	Fe		1.00	-0.94	0.83	0.87	0.90	-0.77	-0.87	0.93	-	0.86	-	0.87	-	-0.69	-0.62	0.97	-	-	0.95	-0.75	0.94	0.88	-0.76	0.94	0.93
	Ca			1.00	-0.78	-0.92	-0.93	0.72	0.86	-0.84	-	-0.84	-	-0.86	-	0.65	0.56	-0.90	-	-	-0.89	0.77	-0.85	-0.86	0.71	-0.88	-0.95
	Mg				1.00	0.81	0.68	-0.74	-0.88	0.73	-	0.61	-0.55	0.94	-	-0.76	-	0.88	0.69	-	0.78	-0.63	0.70	0.56	-0.81	0.87	0.80
	Na					1.00	0.94	-0.88	-0.97	0.80	-	0.76	-0.53	0.82	-	-0.82	-0.64	0.80	-	-	0.90	-0.50	0.71	0.79	-0.91	0.85	0.96
	K						1.00	-0.79	-0.89	0.83	-	0.89	-	0.74	-	-0.66	-0.68	0.81	-	-	0.93	-0.55	0.80	0.92	-0.79	0.84	0.95
	P							1.00	0.92	-0.72	-	-0.58	0.61	-0.65	-	0.95	0.73	-0.69	-	-	-0.82	-	-0.60	-0.63	0.95	-0.81	-0.86
	S								1.00	-0.82	-	-0.73	0.61	-0.83	-	0.88	0.64	-0.82	-	-	-0.89	-	-0.72	-0.72	0.96	-0.88	-0.94
	Ti									1.00	-	0.82	-	0.78	-	-0.67	-0.55	0.85	-	-	0.88	-0.57	0.95	0.83	-0.73	0.85	0.87
	As										1.00	-	0.64	-	-	-	-	0.03	-0.50	-	-	-	-	-			
	Ba											1.00	-	0.64	-	-0.40	-0.56	0.80	-	-	0.82	-0.62	0.88	0.87	-0.59	0.82	0.84
	Cd												1.00	-0.45	-	0.66	0.50	-	-	-	-	-		-	0.73	-	-
	Co													1.00	-	-	-	0.91	0.57	-	0.80	-0.74	0.76	0.67	-0.71	0.81	0.80
	Cr														1.00	-	0.80	-	0.62	-	-	-0.22	-	-	-	-	-
	Cu															1.00	0.58	-0.63	-0.20	0.50	-0.74	-	-	-0.51	0.93	-0.73	-0.78
	Mo																1.00	-0.50	0.15	-	-0.59	-	-	-0.52	0.61	-0.54	-0.61
	Mn																	1.00	0.44	-	0.90	-0.82	-	0.80	-0.69	0.93	0.87
	Ni																		1.00	-	-	-	-	-	-0.28	0.45	-
	Pb																			1.00		-	-	-	-	-	-
	Sc																				1.00	-0.61	0.86	-	-0.84	0.92	0.95
	Sr																					1.00	-0.72	-0.63	0.25	-0.70	-0.59
	V																						1.00	0.85	-0.60	0.87	0.84
	Y																							1.00	-0.63	0.79	0.87
	Zn																								1.00	-0.81	-0.86
	Zr																									1.00	1.00
	Ga																										1.00

($p > 0.05$).

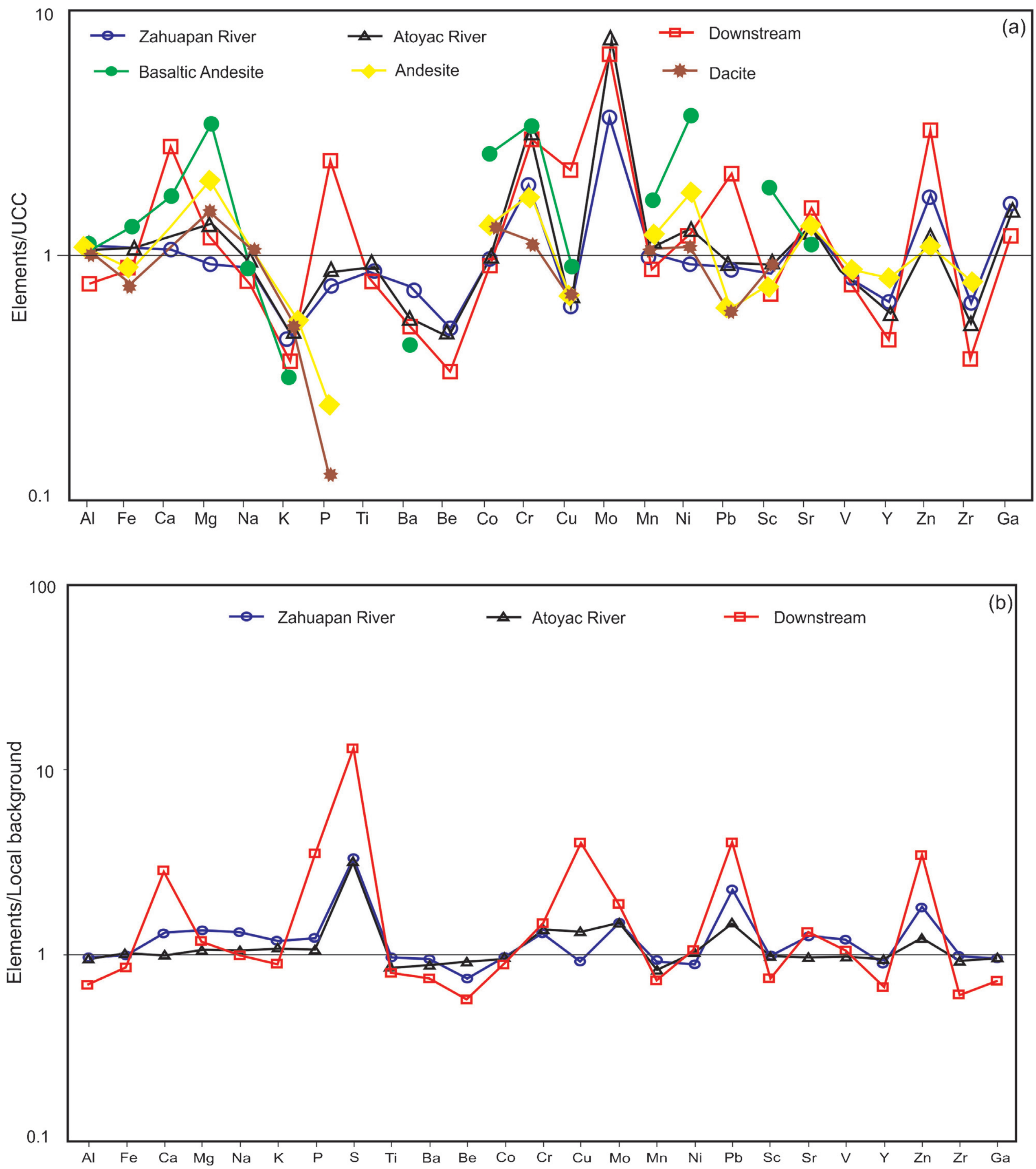

Fig. 4. a–b Multi-element normalized diagram for the sediments of Zahuapan River, Atoyac River and Downstream side, Puebla, México normalized against (a) UCC and (b) background values of the study area.

In the A-CN-K diagram (Fig. 5a), the sediments fall parallel to the A-CN line and are clustered close to plagioclase indicating weak to moderate weathering in the source region. The sediments of Zahuapan River fall slightly away from the feldspar joining line suggesting a moderate weathering condition. In A-CNK-FM ternary plot, most of the samples fall between andesite and feldspar confirming weak to moderate weathering, wherein the sediments are mainly composed of detrital minerals than clay minerals, which is further supported by grain size analysis and ICV values (0.73 to 1.45 for Zahuapan River, 0.93 to 1.52 for Atoyac River and 1.09 to 1.61 for downstream sediments) (Fig. 5b). The sediments show a backward projection of the linear trend in the A-CN-K ternary plot suggesting andesitic-granodiorite source area composition (Fig. 5a). The above inference is very well supported by the A-CNK-FM triangular plot indicating the clustered nature of samples in the same region between feldspar, smectite suggesting that the source area consists of intermediate to mafic (Dacites to basaltic andesites) igneous rock series (Fig. 5b).

The ICV values can be used to distinguish the source rocks and compositional maturity of the sediments (Cox and Lowe, 1995).

Table 4
Factor analysis of three distinct zones from Atoyac River basin sediments, Puebla, Mexico.

Factors/	Factor 1			Factor 2			Factor 3			Factor 4			Factor 5		Factor 6
Elements	RZ	RA	DS	RZ	RA	DS	RZ	RA	DS	RZ	RA	DS	RZ	RA	RZ
Al	−0.71	−0.83	0.63	–	–	–	0.35	–	0.72	–	–	–	–	–	–
Fe	–	0.94	0.83	0.90	–	–	−0.12	–	0.54	–	–	–	–	–	–
Ca	0.83	–	−0.83	–	–	–	0.27	0.64	−0.50	–	–	–	–	–	–
Mg	0.83	0.98	0.59	–	–	−0.52	0.11	–	0.59	–	–	–	–	–	–
Na	0.88	−0.57	0.56	–	–	–	0.14	–	0.79	–	–	–	–	–	–
K	0.85	−0.64	0.67	–	–	–	0.16	–	0.67	–	–	–	–	–	–
P	–	0.56	–	–	–	–	0.08	–	−0.90	–	–	–	–	0.71	0.76
S	–	–	−0.51	–	–	–	−0.06	–	−0.84	0.96	–	–	–	–	–
Ti	–	–	0.73	–	–	–	0.14	–	0.56	–	0.79	–	–	–	−0.74
As	–	–	–	–	0.87	0.80	0.14	–	–	0.88	–	–	–	–	–
Ba	–	–	0.75	–	–	–	−0.27	–	–	–	0.91	–	−0 to 87	–	–
Co	–	0.95	0.72	0.87	–	–	−0.23	–	–	–	–	–	–	–	–
Cr	0.66	–	–	–	0.88	−0.78	0.19	–	–	–	–	–	–	–	–
Cu	–	–	–	–	–	–	–	–	−0.87	0.82	–	–	–	–	–
Mo	–	–	–	−0.70	0.91	–	–	–	−0.72	–	–	–	–	–	–
Mn	–	0.75	0.86	0.73	–	–	–	–	–	–	–	–	–	–	–
Ni	–	0.94	–	0.97	–	−0.86	–	–	–	–	–	–	–	–	–
Pb	–	–	–	–	–	–	0.72	0.85	–	–	–	0.95	–	–	–
Sc	–	0.84	0.72	0.80	−0.52	–	–	–	0.65	–	–	–	–	–	–
Sr	0.88	−0.59	−0.94	–	–	–	–	0.57	–	–	–	–	–	–	–
V	–	–	0.87	–	–	–	0.81	0.91	–	–	–	–	–	–	–
Y	−0.68	–	0.78	–	−0.85	–	–	–	–	–	–	–	–	–	–
Zn	–	–	–	–	–	–	0.96	0.96	−0.92	–	–	–	–	–	–
Zr	–	–	0.76	–	–	–	0.95	0.93	0.57	–	–	–	–	–	–
Ga	−0.87	−0.69	0.71	–	−0.70	–	–	–	0.68	–	–	–		–	–

RZ = River Zahuapan; RA = River Atoyac; DS = Downstream.

Typical rock forming minerals (feldspars, amphiboles and pyroxenes) show ICV values >0.84, whereas typical alteration products such as kaolinite, illite, and muscovite show <0.84 (Cox and Lowe, 1995).The ICV values for the present study ranged from 0.73 to 1.45 for Zahuapan River, 0.93 to 1.52 for Atoyac River and– 1.09 to 1.61 for downstream sediments. The higher ICV values in the present study indicates the dominance of rock forming minerals than the clay minerals which dictates that they are physically eroded, immature and mostly consist of first cycled sediments. Likewise, the downstream sediments show very high ICV values due to higher CaO content. The variations of ICV values can be related to either variation in the source rock composition and/or weathering. The ICV values were plotted against CIA to understand the influence of source rock and weathering (Fig. 6a after Potter et al., 2005). In the plot, most of the samples fall between fresh andesite to granite and nearer to the fresh source rocks indicating weak to moderate weathering and the source rocks mostly being intermediate to felsic in nature. Some of the samples from downstream sediments fall away from the weathering trend due to high CaO content. In addition, the dominance of plagioclase feldspar over K-Feldspar in the sediments is confirmed by K_2O/Na_2O ratio value of <1 in all the studied sediments (Zahuapan River, Atoyac River and downstream) and from the petrographic studies (Dey et al., 2009; Effoudou-Prisoa et al., 2014).

It is well known that transport and deposition of clastic sediments involves mechanical sorting basically fractionating Al_2O_3 (clay minerals) from SiO_2 (quartz and feldspars). Sorting also fractionates TiO_2, mostly present in clay minerals and Ti-oxides, from Zr present in zircon, and sorted with quartz. Ternary plots based on Al_2O_3, TiO_2, and Zr eliminate the weathering effects and may illustrate the presence of sorting-related fractionations which are recognizable by simple mixing trends on a ternary Al_2O_3-TiO_2-Zr diagram (García et al., 1994). The fluvial sediments of Atoyac River basin show a limited range of TiO_2-Zr variations suggesting low compositional maturity and insignificant sorting of the sediments (Fig. 5c). Generally, the Cr/Zr and Zr/Sc ratios increase during the sedimentary process such as sorting and recycling due to accumulation of zircon crystals. Cr/Zr and Zr/Sc ratios in the present study (Cr/Zr = 1.81, 3.20, 7.90 and Zr/Sc = 10.89, 8.21, 7.11 for Zahuapan River, Atoyac River and downstream respectively) suggests no sorting effect (Huntsman-Mapila et al., 2005).

5.3. Provenance

Trace elements such as Sc, Ti, Co, Zr, Hf, Th, and Nb are relatively immobile during surficial processes as they are resistant to chemical weathering and are mostly bound in mineral lattices (Rollinson, 1993). As these elements undergo very little geochemical fractionation, they are used for determining provenance of the sediments in fluvial environment.

In provenance discrimination studies, transitional elements such as Cu, Zn, Pb, Mn, Cr, Fe, and Ni show wide variation in fluvial sediments due to natural effects and contamination during sediment transport/deposition (Li et al., 2001). Al_2O_3/TiO_2 ratios are generally used to trace the source rock composition, since Al mainly hosts in feldspars, whereas Ti in mafic minerals such as olivine, pyroxene, hornblende, biotite, and ilmenite (Hayashi et al., 1997) and thus Al/Ti ratios increases with increasing Si in igneous rocks. According to Hayashi et al. (1997), Al_2O_3/TiO_2 ratios increase as 3–8; 8–21 and 21–70 in mafic, intermediate and felsic igneous source rocks respectively. It is also accepted that this ratio of clastic sedimentary rocks are identical to the parental igneous rocks (Sawyer, 1986; Maynard, 1992; Hayashi et al., 1997). The Al_2O_3/TiO_2 ratio is considered to remain constant during surficial weathering, hydrothermal alteration and volcanic processes and is widely used to identify the source rocks (Hayashi et al., 1997; He et al., 2010; Shao et al., 2016). In the present study, the Al_2O_3/TiO_2 ratios varied from 21.4 to 44.4 for Zahuapan River, 17.5–36.9 for Atoyac River and 14.6–36.2 for downstream sediments indicating that they are derived from intermediate to felsic volcanic source rocks. The source rocks exposed in this region are mainly andesitic to rhyodacitic composition and show Al_2O_3/TiO_2 ratios as 12.46–26.15 for andesites; 16–29 for dacites and 10.93–13.08 for basaltic andesites respectively (Luhr et al., 2006). The studied samples also show that the Al_2O_3/TiO_2 ratios are comparable to the ratios in the source area lithology.

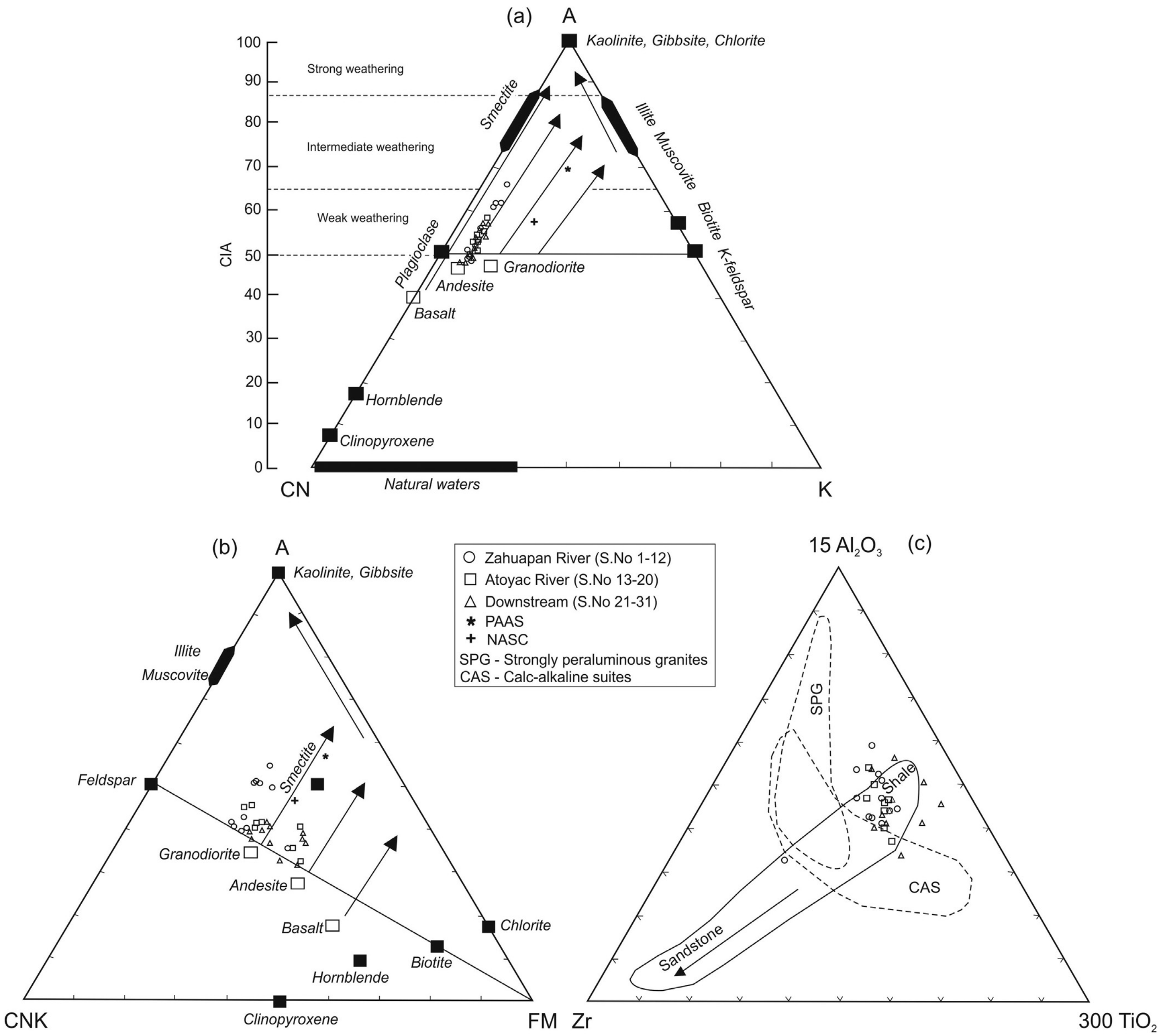

Figure 5. a–c a) A-CN-K, b) A-CNK-FM and c) Al_2O_3-Zr-TiO_2 ternary plots from Zahuapan River, Atoyac River and Downstream side, Puebla, México.

The major element based provenance discrimination diagram by Roser and Korsch (1988) was used to distinguish the provenance characters of the present study since this plot can successfully differentiate the four different provenance areas as mafic, intermediate, felsic and quartzose recycled. Based on the Roser and Korsch (1988) plot, the present study sediments are relatively evolved from intermediate source (Fig. 6b). The samples fall along the magmatic evolution trend from basalt to rhyolite which indicates a typical pattern of first cycle volcanogenic suites (Roser and Korsch, 1988; Purevjav and Roser, 2012). However, few sediment deviated from the magmatic trend due to recycled sediments and more carbonate influences (i.e. in the downstream sediments). Overall, the sediments have undergone little modification of bulk chemistry from the source. The above inference was also confirmed by Ti-Zr diagram of Pearce (1982), where present study samples fall on the boundary line between mafic and felsic provenance area with few samples scattered towards the felsic source (Fig. 6c) suggesting that the source area is dominated by intermediate to felsic arc volcanic rocks. Petrographically the sediments of the study area consist of volcanic (andesite-rhyo-dacite) and pyroclastic (vitric – crystal tuff) fragments as sand grains in addition to the individual mineral grains which are derived from the source region. This is consistent with the geology of the source area and tectonics. Likewise, the lithology of Iztaccihuatl volcano is divided into two main series as older and younger volcanic series (> and <0.6Ma vice versa) (Nixon, 1989). Older series consist of augite hypersthene-pyric lavas and pyroclastic breccias (older andesites and dacites) while younger series mainly consists of hornblende-pyric rocks (younger andesites and dacites) that are differentiated to lavas and pyroclastic breccias. Similarly, lithology of Popocatépetl consists of interlayered lava flows and pyroclastic deposits (andesitic to dacitic composition). Previous studies (Cantagrel et al., 1984; Robin, 1984; Boudal and Robin, 1989; Kolisnik, 1990) indicated that at Popocatépetl volcanic eruptions are the product of mixing and mingling of distinct mafic and silicic magmas. The volcanic and pyroclastic lithics observed in the present study samples are mainly derived from this volcanic region and these sediments are geochemically characterized by intermediate to felsic signature.

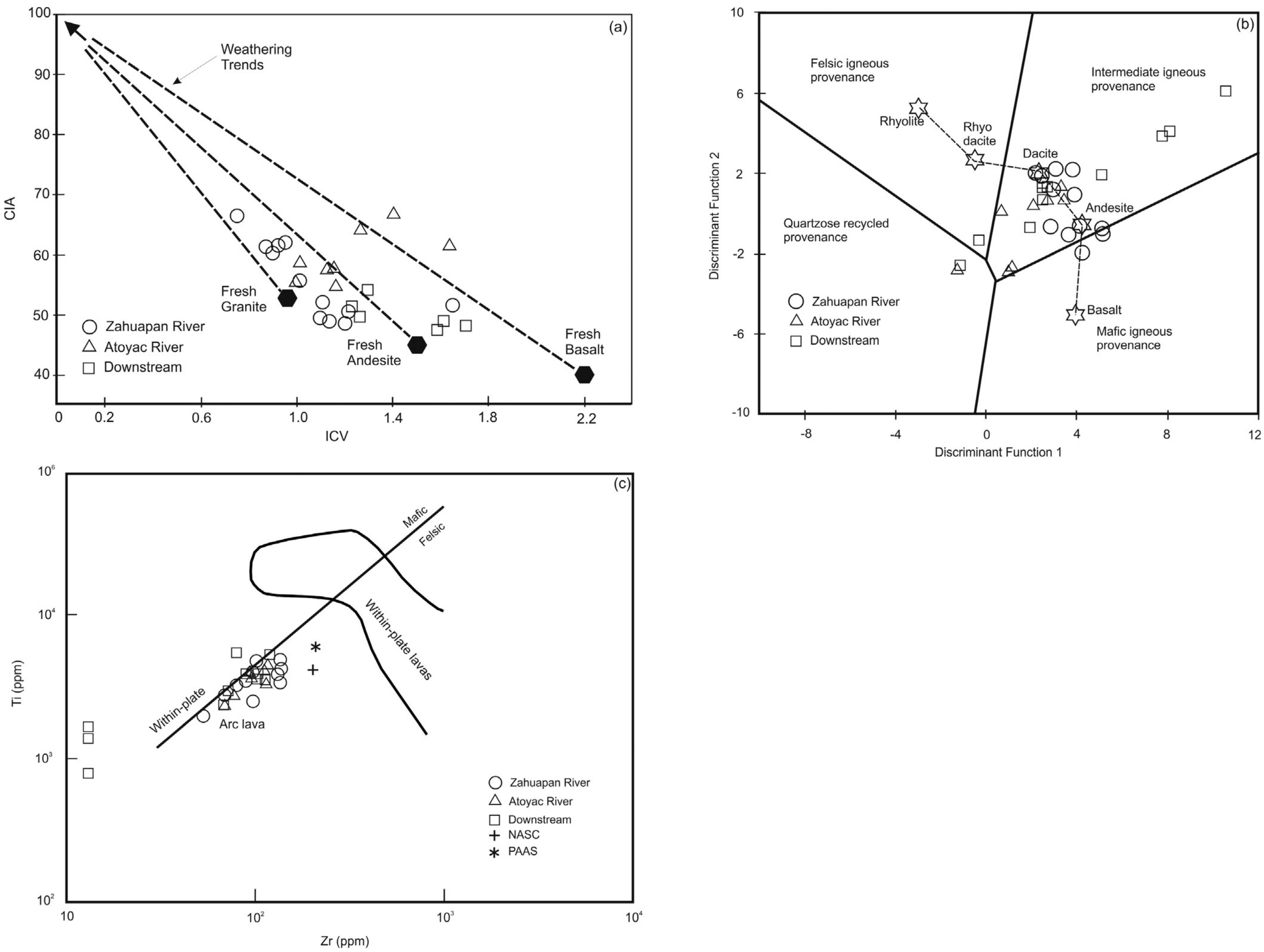

Fig. 6. a–c Source rock identification using scatter plots: a) ICV *vs* CIA b) plot by Roser and Korsch (1988) and c) Ti *vs* Zr for Zahuapan River, Atoyac River and Downstream side sediments, Puebla, México.

The geochemical composition of Cr is a powerful tool in identifying the accessory detrital components like chromite, which are commonly derived from mafic to ultramafic sources including ophiolites (Zimmermann and Bahlburg, 2003). The compatible ferromaganesian trace elements such as Cr, Ni, Co and V have similar behavior in the magmatic processes, but are often fractionated during the weathering process (Feng and Kerrich, 1990; Rollinson, 1993). The higher concentration of Cr (>150 ppm) and Ni (>100 ppm) and their ratio values varies from 1.3 to 1.6 suggesting the presence of ultramafic rocks in the source region (Garver et al., 1996). In the present study, the average Cr and Ni content are (all values in ppm) 189, 37 for Zahuapan River; 314, 58 for Atoyac River and 247, 54 for downstream sediments respectively. The higher content of Cr with higher variation, low content of Ni with limited variation and the high average of Cr/Ni ratios (avg. 4.65, 5.16, 4.60 for R. Zahuapan, R. Atoyac and Downstream side) depict the presence of heavy minerals and anthropogenic input from the local area (in selected samples collected adjacent to City area).

The input of mafic or ultramafic sources could be identified using the Cr/V and Y/Ni ratios (Hiscott, 1984; McLennan, 1993). The Cr/V and Y/Ni ratios in the studied samples are 0.87–3.93 and 0.17–0.54 for Zahuapan River, 1.45–9.49 and 0.18–0.34 for Atoyac River; 0.94–7.85 and 0.08–0.35 for downstream respectively, which shows that only Cr is enriched compared to other ferromagnesian elements. Thus, the enrichment of Cr/Ni (>2) and depletion of Y/Ni values (<1) confirm the presence of heavy minerals such as chromite, which may be derived from mafic source rocks (Young et al., 2013). Cr concentration in Zahuapan River sediments are mainly derived from the source area and are correlated with ferromagnesium minerals such as Mg ($r^2 = 0.89$), Y ($r^2 = 0.70$). However, the elevated concentration of Cr in Atoyac River and downstream sediments are mainly attributed to anthropogenic inputs particularly from steel, chemical, and electroplating industries apart from the natural sources (intermediate volcanic rocks). It is, further confirmed from a strong relationship between Cr with Mg ($r^2 = 0.89$, 0.94), Mo ($r^2 = 0.91$, 0.80) in Atoyac River and downstream sediments, and no or weak correlation of Cr with other ferromagnesium minerals.

5.4. Metal contamination in the fluvial sediments

In order to understand the sediment quality and discern the metal contamination in the fluvial sediments of Atoyac River basin, geochemical normalization of enrichment factor (EF) was widely employed for environmental assessment. The EF values of Zahuapan River sediments suggest a moderate enrichment of S and Pb along with minor enrichment of Zn, Mo, and Cr (Fig. 7a). Atoyac River sediments are moderately enriched with S and minor enrichment of Pb, Mo, Cr and Cu is observed. The downstream sediments displays a minor enrichment of As, Cr, Sr, Ni and V and moder-

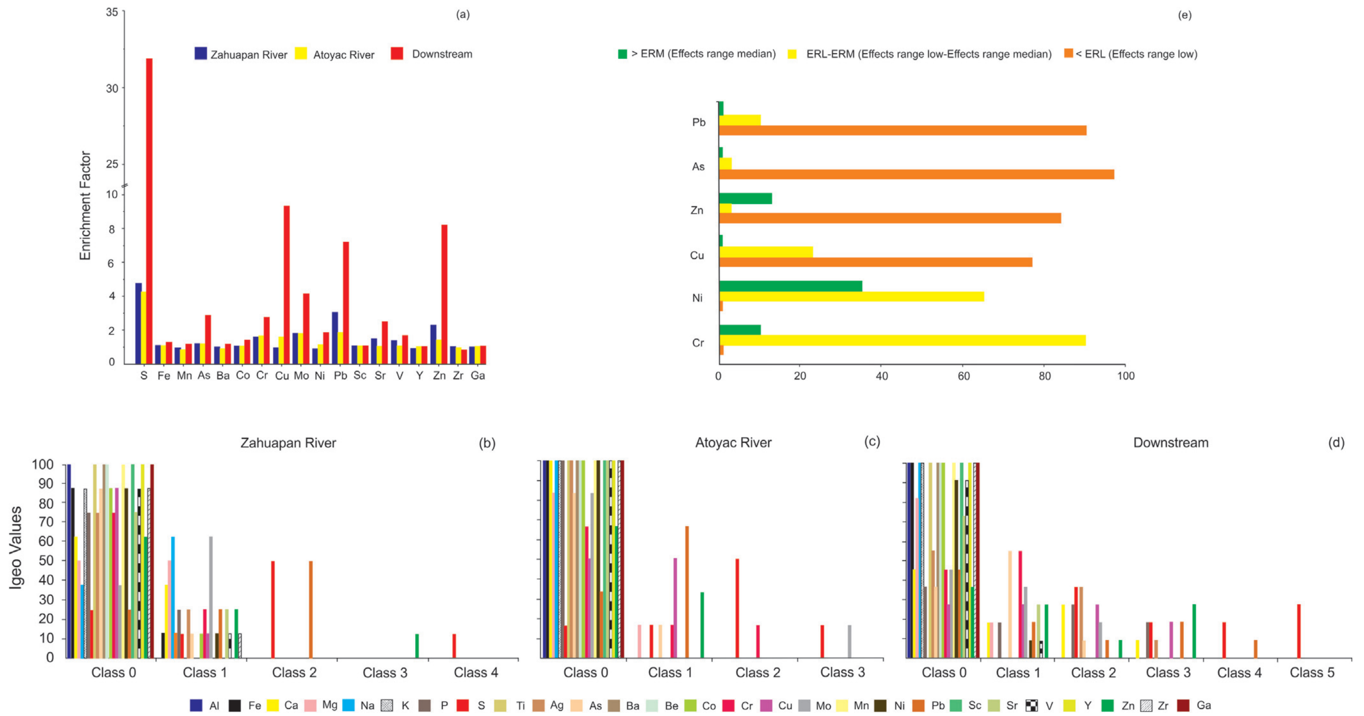

Fig. 7. a–e Metal contamination assessment: a) Enrichment Factor (EF); b–d) I_{geo} values for sediments from Zahuapan River, Atoyac River and Downstream side, Puebla, México and e) potential ecological risk assessment values (ERL/ERM).

ate enrichment of Mo. Significant enrichment of Pb, Cu and Zn as well as very high enrichment of S is observed in the downstream sediments. In all the river samples S is significantly enriched, which is derived from active volcano and its recent volcanic deposits. Among the different zones, the downstream sediments show higher enrichment of metals due to impact of industrial and agricultural effluents derived from the urban zone of Puebla city.

The geoaccumulation index (I_{geo}) is a common geochemical criterion used to evaluate the metal contamination in sediments. The I_{geo} values for Zahuapan River, Atoyac River and downstream sediments are represented in Fig. 7b–d. In Zahuapan River sediments, the I_{geo} values of S and Pb fall in class 2 indicating a moderate contamination and Zn in class 3 with moderate to heavy contamination. Atoyac River sediments consist of S (Class 2 and Class 3), Cr (Class 2) and Mo (Class 3) suggesting moderate to heavily contamination of these elements. Cr and Mo are attributed to the industrial and external inputs from the study area. In the downstream section the elements Ca, P, S, Ag, As, Cu, Mo, Pb, and Zn fall in class 2 and class 3. The higher concentrations of Ca and P in the downstream region is due to the presence of carbonate rocks with Ca bearing minerals such as plagioclase and pyroxenes along with the sewage/industrial effluents and agricultural runoff in this region. The agricultural activities such as application of pesticides, fertilizers and animal manure are the common sources of Cu and Zn (Nicholson et al., 2003; Lu et al., 2012), while Pb is mainly attributed to the automobile exhausts (from primary federal highway) and direct discharges from industries (Micó et al., 2006; Zaborska, 2014). In Atoyac River basin several agricultural practices and presence of waste-water treatment plants has led to significant concentrations of Cu and Zn in the river sediments. The Mexico-Puebla highway, the local road traffic present in the roads that crosses the river basin would probably add to the increased concentrations of Pb in the sediments by surface runoff. A significant enrichment of S is observed in all the three zones, which might be derived from active volcano and its volcanic deposits through atmospheric deposition and runoff respectively.

The calculated PLI values varied from 0.93 to 1.42 for Zahuapan River, 0.94–1.28 for Atoyac River and 0.96–1.51 for downstream sediments and average PLI values for these sediments were 1.15, 1.07 and 1.17, respectively. The above values indicate that the sediments of all the three zones are moderately polluted.

The ecological risk assessment was done on individual samples from the three distinct regions. The results indicate that Cu (77%), Zn (84%), As (97%) and Pb (90%) values were below ERL values (Fig. 7e). It also suggests that more than 75% of the river sediments are not toxic and do not have any ecological risk. All the studied metals such as Cr (90%), Ni (65%), Cu (23%), Zn (3%), As (3%), and Pb (10%) were between ERL and ERM, respectively, indicating relatively less potential ecological risk. In particular, Cr (10%), Ni (35%), and Zn (13%) were higher than the ERM values. Most of these sampling sites which exceeded the ecological risk assessment values were from Atoyac River and downstream section, which received the industrial effluent discharges. Based on this assessment it can be concluded that Cr, Ni and Zn will have an adverse effects on sediment dwelling biota in Atoyac River and downstream sediments (Smolders et al., 2004; Kasprzak and Salnikow, 2007).

6. Conclusion

This study combines texture, petrography, major and trace element geochemistry of the fluvial sediments from Atoyac River basin and yields the following conclusions concerning the provenance, chemical weathering conditions and their potential environmental effects:

- The fluvial sediments of Atoyac River basin are almost entirely of sand and silt sized particles mainly transported by traction mode in both upstream and downstream sections of the river. The petrographic analysis reveals that the sediments are rich in plagioclase, pyroxenes, amphiboles, K-feldspar, biotite, opaque and quartz.

- The geochemical concentrations of these sediments show the characteristics of UCC-like sediments and they are likely derived from a source area with dominant andesitic and dacitic compositions. Based on the concentration pattern, the elements are mainly controlled by either Fe or Mn oxides rather than Al (or clay minerals). The enrichment of some elements (Cu, Zn, Pb, Mn, Cr, Fe, Ni) is due to the presence of active volcano in the upstream side and the industrial corridor in the downstream side of the Atoyac River basin.
- The sediments have undergone weak to moderate weathering as confirmed by CIA, PIA, ICV indices, A-CN-K and A-CNK-FM ternary plots. The results indicate that the fluvial sediments of Atoyac River basin are physically eroded, immature, mostly consist of first cycled sediments and experience a less intense chemical weathering.
- The provenance discrimination diagrams, Al_2O_3/TiO_2, Ti-Zr, Cr/V and Y/Ni ratios suggested that the fluvial sediments were derived from intermediate to felsic volcanic source rocks.
- The enrichment pattern of trace elements (especially Cr, Cu, Pb, Zn, Mo and S) is clearly justified by the higher order of naturally occurring elements and few anthropogenic sources. Cr, Ni and Zn are likely to create adverse effects on sediment dwelling biota based on ecological risk assessment studies.
- The association of elements clearly justifies that mafic input is more from the western side of the study region, where the active volcano (Popocatépetl) is located emitting low level eruptions at regular intervals from past one decade and the vast development of industrial complexes in the Puebla City in Central Mexico also adds to the enrichment pattern.

Acknowledgements

The work is funded by the project "*Estudios para la Red de Estaciones de Monitoreo en Tiempo Real para la Preservación, Conservación y Mejoramiento de la Calidad del Agua en la Cuenca del Alto Atoyac*, Puebla, Mexico and it was financially supported by SDRSOT, Gobierno de Puebla, Mexico. Partial financial support from SIP Project Nos. 20131892 and 20144353 is also highly appreciated. VCS thanks CONACyT for Ph.D Fellowship MPJ, PFRE, DCEU and SSMG wish to express their gratitude to Sistema Nacional de Investigadores (SNI), CONACyT (Mexico), EDI and COFAA (IPN Mexico). Special thanks to Esaú López Martínez and J.S. Wilson.Special thanks to Esaú López Martínez and J.S. Wilson.

References

Ahmad, I., Chandra, R., 2013. Geochemistry of loess-paleosol sediments of Kashmir valley, India: provenance and weathering. J. Asian Earth Sci. 66, 73–89.
Armid, A., Shinjob, R., Zaenia, A., Sanic, A., Ruslan, R., 2014. The distribution of heavy metals including Pb, Cd and Cr in Kendari Bay surficial sediments. Mar. Pollut. Bull. 84, 373–378.
Armstrong-Altrin, J.S., Nagarajan, R., Balaram, V., Natalhy-Pineda, O., 2015. Petrography and geochemistry of sands from the Chachalacas and Veracruz beach areas, western Gulf of Mexico, Mexico: constraints on provenance and tectonic setting. J. South Am. Earth Sci. 64, 199–216.
Bhatia, M.R., 1983. Plate tectonics and geochemical composition of sandstones. Geology 91, 611–627.
Bhuiyan, M.A.H., Rahman, M.J.J., Dampare, S.B., Suzuki, S., 2011. Provenance, tectonics and source weathering of modern fluvial sediments of the Brahmaputra-Jamuna River, Bangladesh: inference from geochemistry. J. Geochem. Explor. 111, 113–137.
Blott, S.J., Pye, K., 2001. GRADISTAT: a grain size distribution and statistics package for the analysis of unconsolidated sediments. Earth Surf. Processes Landforms 26, 1237–1248.
Bock, B., McLennan, S.M., Hanson, G.N., 1998. Geochemistry and provenance of the middle ordovician Austin glen member (Normanskill formation) and the taconian orogeny in new england. Sedimentology 45, 635–655.
Boudal, C., Robin, C., 1989. Volcan Popocatépetl: recent eruptive history, and potential hazards and risks in future eruptions. In: Latter, J.H. (Ed.), Volcanic Hazards, International Association of Volcanology and Chemistry of the Earth's Interior Proceedings in Volcanology, vol. 1. Springer Verlag, Berlin, pp. 110–128.
Buat-Ménard, P., Chesselet, R., 1979. Variable influence of the atmospheric flux on the trace metal chemistry of oceanic suspended matter. Earth Planet. Sci. Lett. 42, 398–411.
CONAGUA, 2010. Estadísticas del Agua en México, edición 2010. 10 años de presentar al agua en cifras. México D.F.: Secretaría de Medio Ambiente y Recursos Naturales. http://www.atl.org.mx/index.php?option=com_content&view=article&id=1990:estadisticas-delagua-en-mexico-edicio2010&catid=48:datoestadicos&Itemid=478 Accessed March 23, 2016.
Calvert, S.E., Pedersen, T.F., Karlin, R.E., 2001. Geochemical and isotopic evidence for post-glacial palaeoceanographic changes in Saanich Inlet, British Columbia. Mar. Geol. 174, 287–305.
Cantagrel, J.M., Gourgaud, A., Robin, C., 1984. Repetitive mixing events and Holocene pyroclastic activity at Pico de Orizaba and Popocatepetl (Mexico). Bull. Volcanol. 47 (4), 735–748.
Carver, R.E., 1971. Procedures in Sedimentary Petrology. John Wiley and Sons, Canada, Limited, New York, pp. 653.
Castro-Goeva, R., 1999. Historia eruptiva reciente del volcán La Malinche. Tesis de Maestría. Instituto de Geofísica, Posgrado de Geofísica. Instituto de Geofísica, Posgrado de Geofísica, UNAM, México.
Castro-Govea, R., Siebe, C., 2007. Late PleistoceneeHolocene stratigraphy and radiocarbon dating of La Malinche volcano, central Mexico. J. Volcanol. Geotherm. Res. 162, 20–42.
Cervantes, P., Wallace, P., 2003. Role of water in subduction zone magmatism: new insights from melt inclusion in high-Mg basalt from Central Mexico. Geology 31, 235–238.
Chen, H., Teng, Y., Li, J., Wu, J., Wang, J., 2016. Source apportionment of trace metals in river sediments: a comparison of three methods. Environ. Pollut. 211, 28–37.
Covelli, S., Fontolan, G., 1997. Application of a normalization procedure in determining regional geochemical baselines. Env. Geol. 30 (1/2), 34–45.
Cox, R., Lowe, D.R., 1995. A conceptual review of regional – scale controls on the composition of clastic sediment and the co-evolution of continental blocks and their sedimentary cover. J Sed. Res. 65, 1–21.
Cullers, R.L., Basu, A., Suttner, L.J., 1988. Geochemical signature of provenance in sand size material in soils and stream sediments near the Tobacco Root batholith Montana, USA. Chem. Geol. 70, 335–348.
D'Oriano, C., Bertagnini, A., Cioni, R., Pompilio, M., 2014. Identifying recycled ash in basaltic eruptions. Sci. Rep. 4, 5851, http://dx.doi.org/10.1038/srep05851.
Dey, S., Rai, A.K., Chaki, A., 2009. Palaeoweathering, composition and tectonics of provenance of the Proterozoic intracratonic Kaladgi-Badami basin, Karnataka, southern India: evidence from sandstone petrography and geochemistry. J. Asian Earth Sci. 34, 703–715.
Effoudou-Prisoa, E.N., Onana, V.L., Boubakar, L., Beyala, V.K.K., Ekodeck, G.E., 2014. Relationships between major and trace elements during weathering processes in a sedimentary context: implications for the nature of source rocks in Douala, Littoral Cameroon. Chemie der Erde 74, 765–781.
Erffa von, A., Hilger, W., Knoblich, K.L., Weyl, R., 1976. Geología de la Cuenca Alta de Puebla-Tlaxcala y sus contornos, vol. 13. Comunicaciones Proyecto Puebla Tlaxcala, México, pp. 99–116.
Farhat, H.I., Salem, S.G., 2015. Effect of flooding on distribution and mode of transportation of Lake Nasser sediments, Egypt. Egypt. J. Aquat. Res., http://dx.doi.org/10.1016/j.ejar.2015.03.009.
Fedo, C.M., Nesbitt, H.W., Young, G.M., 1995. Unraveling the effects of potassium metasomatism in sedimentary rocks and paleosols: with implications for paleoweathering conditions and provenance. Geology 23, 921–924.
Fedo, C.M., Eriksson, K.A., Krogstad, E.J., 1996. Geochemistry of shales from the Archean (3.0 Ga) Buhwa Greenstone Belt, Zimbabwe: implications for provenance and source-area weathering. Geochim. Cosmochim. Acta 60, 1751–1763.
Feng, R., Kerrich, R., 1990. Geochemistry of fine-grained clastic sediments in the Archean Abitibi greenstone belt, Canada: implications for provenance and tectonic setting. Geochim. Cosmochim. Acta 54, 1061–1081.
Folk, R.L., 1980. Petrology of Sedimentary Rocks. Hemphills Publ Co., Austin, Texas, pp. 170.
Friedman, G.M., 1961. Distinction between dune: beach and river sands from textural characteristics. J. Sed. Petrol. 31, 514–529.
García, D., Fonteilles, M., Moutte, J., 1994. Sedimentary fractionations between Al, Ti, and Zr and the genesis of strongly prealuminous granites. J. Geol. 102, 411–422.
Garver, J.I., Royce, P.R., Smick, T.A., 1996. Chromium and nickel in shale of the Taconic foreland: a case study for the provenance of fine-grained sediments with an ultramafic source. J. Sed. Res. 100, 100–106.
Glasby, G.P., Szefer, P., Geldon, J., Warzocha, J., 2004. Heavy-metal pollution of sediments from Szczecin Lagoon and the Gdansk Basin. Poland.Sci. Total Environ. 330, 249–269.
Goff, F., Love, S.P., Warren, R.G., Counce, D., Obenholzner, J., Siebe, C., Schmidt, C., 2001. Passive infrared remote sensing evidence for large intermittent CO2 emissions at Popocatepetl volcano, Mexico. Chem. Geol. 177, 133–156.
Griffiths, J.C., 1951. Size versus sorting in Caribbean sediments. J. Geol. 59, 211–243.
Hanif, N., Shah Eqani, S.A.M.A., Ali, S.M., Cincinelli, A., Ali, N., Katsoyiannis, I.A., Tanveer, Z.I., Bokhari, H., 2016. Geo-accumulation and enrichment of trace metals in sediments and their associated risks in the Chenab River, Pakistan. J. Geochem. Explor. 165, 62–70.
Hayashi, Ken-I., Fujisawa, H., Holland, H.D., Ohmoto, H., 1997. Geochemistry of 1.9 Ga sedimentary rocks from northeastern Labrador, Canada. Geochim. Cosmochim. Acta 61, 4115–4137.

He, Z.Y., Xu, X.S., Zou, H.B., Wang, X.D., Yu, Y., 2010. Geochronology, petrogenesis and metallogeny of Piaotang granitoids in the tungsten deposit region of South China. Geochem. J. 44, 299–313.
Hiscott, R.N., 1984. Ophiolitic source rocks for Taconic-age flysch: trace element evidence. Geol. Soc. Am. Bull. 95, 1261–1267.
Huntsman-Mapila, P., Kampunzu, A.B., Vink, B., Ringrose, S., 2005. Cryptic indicators of provenance from the geochemistry of the Okavango Delta sediments, Botswana. Sed. Geol. 174, 123–148.
INEGI, 1981. Síntesis Geográfica De Tlaxcala. SSP, México, pp. 14–16.
INEGI, 2010. Censo de Población y Vivienda, 2010. http://www.censo2010.org.mx Accessed March 23, 2016.
Johnsson, M.J., Meade, R.H., 1990. Chemical weathering of fluvial sediments during alluvial storage; the Macuapanim Island point bar, Solimões River, Brasil. J. Sediment. Petrol. 60, 827–842.
Kalender, L., Uçar, S.C., 2013. Assessment of metal contamination in sediments in the tributaries of the Euphrates River, using pollution indices and determination of the pollution source, Turkey. J. Geochem. Explor. 134, 73–84.
Kasprzak, K.S., Salnikow, K., 2007. Nickel toxicity and carcinogenesis. In: Siegel, A., Siegel, H., Siegel, R.K.O. (Eds.), Metal Ions in Life Science, vol. 2. Wiley, Chichester, pp. 619–660.
Khalifa, I.H., El-Bialy, M.Z., Hassan, D.M., 2011. Petrologic and geochemical characterization and mineralization of the metavolcanic rocks of the Heib Formation, Kid Metamorphic Complex, Sinai, Egypt. Geosci. Front. 2 (3), 385–402.
Kolisnik, A.M., 1990. Phenocryst Zoning and Heterogeneity in Andesites and Dacites of Volcán Popocatépetl, México [M.S. Thesis]. Queen's University, Kingston, Ontario, Canada, pp. 247.
Krippner, S.J.P., Briggs, R.M., Wilson, C.J.N., Cole, J.W., 1998. Petrography and geochemistry of lithic fragments in ignimbrites from the Mangakino Volcanic Centre: implications for the composition of the subvolcanic crust in western Taupo Volcanic Zone New Zealand. N. Z. J. Geol. Geophys. 41 (2), 187–199.
Larocque, A.C.L., Stimac, J.A., Siebe, C., Greengrass, K., Chapman, R., Mejia, S.R., 2008. Deposition of a high-sulfidation Au assemblage from a magmatic volatile phase volcán Popocatépetl, Mexico. J. Vol. Geother. Res. 170, 51–60.
Li, X.D., Poon, C.S., Liu, P.S., 2001. Heavy metal contamination of urban soils and street dusts in Hong Kong. App. Geochem. 16, 1361–1368.
Liu, B., Wang, Y., Su, X., Zheng, H., 2013. Elemental geochemistry of northern slope sediments from the South China Sea: implications for provenance and source area weathering since Early Miocene. Chem. Erde 73, 1–7.
Long, E.R., MacDonanld, D.D., Smith, S., Calder, F., 1995. Incidence of adverse biological effects within ranges of chemical concentrations in marine and estuarine sediments. Environ. Manage. 19, 81–97.
Lu, A., Wang, J., Qin, X., Wang, K., Han, P., Zhang, S., 2012. Multivariate and geostatistical analyses of the spatial distribution and origin of heavy metals in the agricultural soils in Shunyi Beijing, China. Sci. Total Environ. 425, 66–74.
Luhr, J.F., Kimberly, P., Siebert, L., Aranda-Gómez, J.J., Housh, T.B., Kysar Mattietti, G., 2006. Mexico's Quaternary volcanic rocks: insights from the MEXPET petrological and geochemical database. In: Siebe, C., Macías, J.L., Aguirre-Díaz, G.J. (Eds.), Neogene-Quaternary Continental Margin Volcanism: A Perspective from Mexico, vol. 402. Geol. Soc. of America Spl. Paper., pp. 1–44.
Maynard, J.B., 1992. Chemistry of modern soils as a guide to interpreting Precambrian paleosols. J. Geol. 100, 279–289.
McLennan, S.M., 1993. Weathering and global denudation. J. Geol. 101, 295–303.
Micó, C., Recatala, L., Peris, M., Sanchez, J., 2006. Assessing heavy metal sources in agricultural soils of an European Mediterranean area by multivariate analysis. Chemosphere 65, 863–872.
Muller, G., 1981. The heavy metal pollution of the sediments of Neckars and its tributary: a stocktaking. Chem. Zeit. 105, 157–164.
Nagarajan, R., Roy, P.D., Jonathan, M.P., Lazano, R., Kessler, F.L., Prasanna, M.V., 2014. Geochemistry of Neogene sedimentray rocks from Borneo Basin, East Malaysia: paleo-weathering, provenance, and tectonic setting. Chem. Erde Geochem. 74 (1), 139–146.
Naimo, D., Adamo, P., Imperato, M., Stanzione, D., 2005. Mineralogy and geochemistry of a marine sequence, Gulf of Salerno, Italy. Quatern. Int. 140–141, 53–63.
National Meteorological Service, 2010. http://smn.cna.gob.mx/index.php?option=com content&view=article&id=12&Itemid=77.
Nehyba, S., Roetzel, R., 2015. Depositional environment and provenance analyses of the zobing formation (Upper carboniferous-Lower permian), Austria. Aust. J. Earth Sci. 108 (2), 245–276.
Nelson, S.T., Montana, A., 1992. Sieve-textured plagioclase in volcanic rocks produced by rapid decompression. Am. Mineral. 77, 1242–1249.
Nelson, S.A., Sanchez-Rubio, G., 1986. Trans Mexican Volcanic Belt Field Guide. Volcanology Division, Geological Association of Canada.
Nesbitt, H.W., Young, G.M., 1982. Early Proterozoic climates and plate motions inferred from major element chemistry of lutites. Nature 299, 715–717.
Nesbitt, H.W., Young, G.M., 1984. Prediction of some weathering trends of plutonic and volcanic rocks based on thermodynamic and kinetic considerations. Geochim. Cosmochim. Acta 48, 1523–1534.
Nesbitt, H.W., Young, G.M., 1989. Formation and diagenesis of weathering profiles. J. Geol. 97, 129–147.
Nesbitt, H.W., Markovics, G., Price, R.C., 1980. Chemical processes affecting alkalis and alkaline earths during continental weathering. Geochim. Cosmochim. Acta 44, 1659–1666.
Nicholson, F.A., Smith, S.R., Alloway, B.J., Carlton-Smith, C., Chambers, B.J., 2003. An inventory of heavy metals inputs to agricultural soils in England and Wales. The Sci. Total Environ. 311, 205–219.
Nixon, G., 1989. The geology of Iztaccíhuatl volcano and adjacent areas of the Sierra Nevada and valley of Mexico. Geol. Soc. Am. Special Paper 219.
Obenholzner, J.H., Schroettner, P.G., Delgado, H., 2003. Particles from the plume of Popacatépetl volcano, Mexico – FESEM/EDS approach. In: Oppenheimer, C., Pyle, D.M., Barclay, J. (Eds.), Volcanic Degassing, vol. 213. Geol. Soc. London, pp. 123–148.
Okeyode, I.C., Jibiri, N.N., 2013. Grain size analysis of the sediments from Ogun river, south western Nigeria. Earth Sci. Res., http://dx.doi.org/10.5539/esr.v2n1p43.
Pe-Piper, G., Pe-Piper, D.J.W., Dolansky, L.M., 2005. Alteration of ilmenite in the cretaceous sands of nova scotia, southeastern Canada. Clays and Clay Min. 53, 490–510.
Pearce, J.A., 1982. Trace element characteristics of lavas from destructive plate boundaries. In: Thorpe, R.S. (Ed.), Andesites. Wiley, Chichester, pp. 525–548.
Potter, P.E., Maynard, J.B., Depetris, P.J., 2005. Mud and Mudstones: Introduction and Overview. Springer-Verlag, Heidelberg, pp. 297.
Purevjav, N., Roser, B., 2012. Geochemistry of Devonian-Carboniferous clastic sediments of the Tsetserleg terrane, Hangay Basin, Central Mongolia: provenance, source weathering, and tectonic setting. Isl. Arc 21, 270–287.
Ramírez Rojas, O., 1986. Estudio geológico preliminar para el proyecto de presa ayehualco temezontla, mpio. panotla, tlax. tesis de doctorado. Instituto de geologia UNAM.
Robin, C., 1984. Le volcan Popocatépetl (Mexique) Structure, evolution pétrologique et risques. Bull. Volcanol. 47, 1–23.
Rollinson, H.R., 1993. Using Geochemical Data: Evaluation, Presentation, Interpretation. Routledge, United Kingdom.
Roser, B.P., Korsch, R.J., 1988. Provenance signatures of sandstone-mudstone suites determined using discriminant function analysis of major-element data. Chem. Geol. 67, 119–139.
Rubio, B., Nombela, M.A., Vilas, F., 2000. Geochemistry of major and trace elements in sediments of the Ria de Vigo (NW Spain): an assessment of metal pollution. Mar. Pollut. Bull. 40 (11), 968–980.
Sakan, S.M., Djordjevic, D.S., Manojlovic, D.D., Polic, P.S., 2009. Assessment of heavy metal pollutants accumulation in the Tisza River sediments. J. Environ. Manage. 90 (11), 3382–3390.
Sawyer, E.M., 1986. The influence of source rock type, chemical weathering and sorting on the geochemistry of clastic sediments from Quetico metasedimentary belt Superior Province. Canada.Chemical Geol. 55, 77–95.
Schaaf, P., Stimac, J., Siebe, C., Macías, J.L., 2005. Geochemical evidence for mantle origin and crustal processes in volcanic rocks from Popocatépetl and surrounding monogenetic volcanoes, Central Mexico. J. Petrol. 46, 1243–1282.
Schmitz, M.D., Smith, I.E.M., 2004. The petrology of the rotoiti eruption sequence, taupo volcanic zone: an example of fractionation and mixing in a rhyolitic system. J. Petrol. 45 (10), 2045–2066.
Schneider, S., Hornung, J., Hinderer, M., Garzanti, E., 2016. Petrography and geochemistry of modern river sediments in an equatorial environment (Rwenzori Mountains and Albertine rift: uganda) – implications for weathering and provenance. Sed. Geol. 336, 106–119.
Shao, L., Cao, L., Pang, X., Jiang, T., Qiao, P., Zhao, M., 2016. Detrital zircon provenance of the Paleogene syn-rift sediments in the northern South China Sea. Geochem. Geophys. Geosyst., http://dx.doi.org/10.1002/2015gc006113.
Sharma, A., Sensarma, S., Kamlesh, K., Khanna, P.P., Saini, N.K., 2013. Mineralogy and geochemistry of the Mahi River sediments in tectonically active western India Implications for Deccan large igneous province source, weathering and mobility of elements in a semi-arid climate. Geochim. Cosmochim. Acta. 104, 63–83.
Siebe, C., Macías, J.L., 2004. Volcanic hazards in the Mexico City metropolitan área from eruptions at Popocatépetl, Nevado de Toluca and Jocotitlán stratavolcanoes and monogenetic scoria cones in the Sierra Chichinautzin volcanic field. In: Field Guide, Penrose Conference, Neogene-Quaternary Continental Margin Volcanism, Jan 2004, State of Puebla, Mexico. Boulder, CO. Geol Soc. Amer, p. 77.
Siebe, C., Abrams, M., Macías, J.L., Obenholzner, J., 1996. Repeated volcanic disasters in Prehispanic time at Popocatépetl, Central México: past key to the future? Geology 24 (5), 399–402.
Smolders, E., Buekers, J., Oliver, I., McLaughlin, M.J., 2004. Soil properties affecting toxicity of zinc to soil microbial properties in laboratory-spiked and field-contaminated soils. Environ. Toxicol. Chem. 23, 2633–2640.
Stevens, R.E., Metcalfe, S.E., Leng, M.J., Lamb, A.L., Sloane, H.J., Naranjo, E., González, S., 2012. Reconstruction of Late Pleistocene climate in the Valsequillo Basin (Central Mexico) through isotopic analysis of terrestrial and freshwater snails. Paleogeo. Paleoclim. Paleoecol. 319–320, 16–27.
Takarina, N.D., 2010. Geochemical fractionation of toxic trace heavy metals (Cr, Cu, Pb, and Zn) from the estuarine sediments of 5 river mouths at Jakarta Bay, Indonesia. J. Coast. Dev. 13, 26–36.
Tomlinson, D.L., Wilson, J.G., Harris, C.R., Jeffrey, D.W., 1980. Problems in the assessment of heavy-metal levels in estuaries and the formation of a pollution index. Helgoländer Meeresuntersuchungen 33 (1–4), 566–575.
United States Environmental Protection Agency (USPEA), 2001. The Role of Screening Level Risk Assessments and Refining Contaminants of Concern in Baseline Ecological Risk Assessments publications. 9345-014, EPA 540/F-01/14, June 2001.

Van Loon, A.J., Mange, A.M., 2007. In situ dissolution of heavy minerals through extreme weathering, and the application of the surviving assemblages and their dissolution characteristics to correlation of dutch and german silver sands. In: Mange, M.A., Wright, D.T. (Eds.), Heavy Minerals in Use Developments in Sedimentology Series, vol 58. Elsevier, Amsterdam, pp. 189–213.
Visher, G.S., 1969. Grain size distribution and depositional processes. J. Sediment Petrol. 39, 1074–1106.
Wei, G., Liu, X.H., Liu, Y., Shao, L., Liang, X., 2006. Geochemical record of chemical weathering and monsoon climate change since the early Miocene in the South China Sea. Paleoceanography 21, 4214–4225.
Weidendorfer, D., Mattsson, H.B., Ulmer, P., 2014. Dynamics of magma mixing in partially crystallized magma chambers: textural and petrological constraints from the basal complex of the austurhorn intrusion (SE Iceland). J. Petrol 55 (9), 1865–1903.
Witter, J.B., Kress, V.C., Newhall, C.G., 2005. Volcán popocatepetl, Mexico. Petrology, magma mixing, and immediate sources of volatiles for the 1994-present eruption. J. Petrol 46 (11), 2337–2366.
Wronkiewicz, D.J., Condie, K.C., 1987. Geochemistry of Archean shales from the Witwaterstrand Supergroup, South Africa: source area weathering and provenance. Geochim. Cosmochim. Acta 51, 2401–2416.
Young, S.M., Pitawala, A., Ishiga, H., 2013. Geochmeical characteristics of stream sediments, sediment fractions, soils and basement rocks from the Mahaweli River and its catchment, Sri Lanka. Chem. Erde 73, 357–371.
Zaborska, A., 2014. Anthropogenic lead concentrations and sources in Baltic Sea sediments based on lead isotopic composition. Mar. Pollut. Bull. 85, 99–113.
Zhang, J., Liu, C.L., 2002. Riverine composition and estuarine geochemistry of particulate metals in China-weathering features: anthropogenic impact and chemical fluxes. Estuar. Coast. Shelf. Sci. 54, 1051–1070.
Zimmermann, U., Bahlburg, H., 2003. Provenance analysis and tectonic setting of the Ordovician clastic deposits in the southern Puna Basin, NW Argentina. Sedimentology 50, 1079–1104.